Tuning mTORC1 activity dictates the response of acute myeloid leukemia to LSD1 inhibition

Amal Kamal Abdel-Aziz,[1,2] Isabella Pallavicini,[1] Elena Ceccacci,[1] Giuseppe Meroni,[3] Mona Kamal Saadeldin,[1,4] Mario Varasi[3] and Saverio Minucci[1,5]

[1]Department of Experimental Oncology, IEO, European Institute of Oncology IRCCS, Milan, Italy; [2]Department of Pharmacology and Toxicology, Faculty of Pharmacy, Ain Shams University, Cairo, Egypt; [3]Experimental Therapeutics IFOM-FIRC Institute of Molecular Oncology Foundation, Milan, Italy; [4]Faculty of Biotechnology, October University for Modern Sciences and Arts, 6th October City, Cairo, Egypt and [5]Department of Biosciences, University of Milan, Milan, Italy

©2020 Ferrata Storti Foundation. This is an open-access paper. doi:10.3324/haematol.2019.224501

Received: April 19, 2019.

Accepted: September 16, 2019.

Pre-published: September 19, 2019.

Correspondence: *SAVERIO MINUCCI* - saverio.minucci@ieo.it

Supplemental Methods

Reagents

DDP38003 (referred to as Compound 15) was synthesized as described before.[1] MC2805 (Compound 14e in [2]) was kindly provided by Prof. Antonello Mai. Rapamycin (Sirolimus)(Catalog.No.R-5000) was purchased from LC laboratories. AZD8055 (Catalog.No.S1555) and U0126 (Catalog.No.S1102) were purchased from Selleckchem.2-Deoxy-D-glucose(Catalog.No.D8375), all-trans-retinoic acid (Catalog.No.R2625), May-Grunwald, Giemsa and ROCHE Complete™ EDTA-free Protease Inhibitor Cocktail (Catalog.No.11836170001)were purchased from Sigma Aldrich. NT-157 (Catalog.No.23442) was purchased from Cayman. Bio-Rad DC™ Protein Assay (Catalog.No.500-0114) was purchased from Biorad.

Antibodies

Primary antibodies against p-mTOR (S2448) (5536), total mTOR (2972), p-p70 S6K (T389) (9234), total p70 S6K, pS6 (S235/236) (2211), total S6 (54D2), p-4E-BP1 (T37/46) (2855), total 4E-BP1 (9644), p-AKT (S473) (9271), total AKT (9272), p-AMPK, total AMPK, p-acetyl CoA carboxylase, total acetyl CoA carboxylase (3676), p-ERK1/2 (T202/Y204) (4370), total ERK1/2 (4695), raptor (24C12), IRS1 (2382S) and LSD1 (2139) were purchased from Cell Signaling Technology. H3K4me2 (ab32356), H3K4me3 (ab8580), H3K27Ac (ab4729) and LSD1 (ab17721) antibodies were purchased from Abcam. H3K9Ac antibody was purchased from Diagenode. Antibodies against vinculin and β-actin were purchased from Sigma Aldrich. Rabbit IgG was purchased from Jackson Immunoresearch Labs Inc. Anti-human CD45 PerCP (345809) was purchased from BD Biosciences. Anti-human nuclei (4383) was purchased from Millipore.

Cell proliferation and ATP Cell Titer Glo™ assays

AML cells were cultured in T175 flasks and treated as indicated. Cell counts were performed in triplicates using trypan blue (0.2%) to identify viable AML cells using Biorad TC20™ automated cell counter. Unless otherwise specified, AML cells were cultured and treated in 96-well plate as indicated and their ATP levels were then determined using a Cell Titer-Glo™ assay (Promega Corporation, USA). Luminescence was measured using Glomax™ Multi-Detection System.

Retroviral constructs and retroviruses production

shRNA constructs were prepared in the MSCV-based pLMP retroviral vector as previously described[1]. The hairpins used in the study are outlined in Table.S6. Supernatants from transfected Phoenix packaging cells were collected 48 and 72 h post-transfection and immediately used for infection cycles.

Retroviral transduction of AML cells

For transducing THP-1, OCI-AML3 and KASUMI-1 cells, cells were diluted in retroviral supernatants added with 8µg/mL polybrene and seeded in 24-well plate. Spin infection was performed for 2 consecutive days (2 cycles of infection/day) at 1800 *rpm* for 45 min. For THP-1 and OCI-AML3 cells, puromycin selection was initiated 24 h after the last cycle of infection. Early passages of puromycin-resistant pool of cells were used for subsequent experiments. For KASUMI-1 cells, GFP positive cells were sorted and used for subsequent experiments.

Establishment of LSD1i-resistant AML cells

To generate LSD1i-resistant cells, parental LSD1i-naïve/responsive KASUMI-1 cells (designated KASUMI-1/P) were continuously exposed to increasing concentrations of DDP38003 as previously described[3]. After twelve months, descendent KASUMI-1 cells started to grow and proliferate in the presence of DDP38003. The derived resistant cells were named KASUMI-1/R cells. Resistance index (RI) was determined as the ratio of the median inhibitory concentration (IC_{50}) of KASUMI-1/R subline divided by the IC_{50} of KASUMI-1/P. Cross resistance of KASUMI-1/R cells to varying concentrations of MC2580 was confirmed using Cell Titer-Glo™ Luminescent assay.

Western blot analysis

Cells were washed and then lysed in HEPES lysis buffer supplemented with protease/phosphatase inhibitor cocktail as previously described[4]. After 20 min incubation on ice, cell lysates were centrifuged at 14,000 *rpm* for 10 min at 4°C. Cell lysates were resolved onto 12% SDS-PAGE and proteins were transferred to nitrocellulose membranes (Protran BA85, GE Healthcare life sciences) and then blocked for 1 h at using 5% skimmed milk in TBST. Incubation with the specific primary antibodies was performed in blocking buffer at 4°C. Horseradish peroxidase-conjugated anti-IgG was used as secondary antibody.

Immunoreactive bands were detected by ECL chemiluminescent substrate (Amersham ECL Prime Western Blotting Detection Reagent, GE Healthcare life sciences).

Apoptosis detection using Annexin V/PI staining

Extent of apoptosis in untreated and treated AML cells was assessed using Annexin V/ Propidium iodide (PI) assay as previously described[5]. Data were analyzed using FlowJo software.

Cell cycle analysis

Briefly, following the treatment of AML cells as indicated, cells were fixed in 70% ethanol and treated with RNAse and stained with PI overnight before FACS analysis was carried out as previously indicated [6]. Data were analyzed using FlowJo software.

Real time-reverse transcriptase quantitative PCR (RT-qPCR)

RNA was extracted from the cells using RNA extraction kit (Direct-zol™ RNA kit, Zymo research Corp). RNA quantity was evaluated spectrophotometrically using NanoDrop (ND-1000 Technologies Inc.). cDNA was used to carry out quantitative PCR using SYBR Green Reaction Mix (Perkin Elmer, Boston, MA). mRNA levels were normalized against the house keeping gene (GAPDH) mRNA. The sequences of the primers used in the present study are listed in Table.S7.

RNA-Sequencing and bioinformatic analysis

Cells were pelleted and RNA was isolated using an RNA extraction kit (Direct-zol™ RNA kit, Zymo research Corp). RNA-seq libraries were constructed using the Illumina TruSeq RNA sample preparation protocol. Single-end reads were aligned to the *hg18* reference genome using TopHat v2.0.13 [7] with default parameters, except for using the option *--no-coverage-search*. The normalized coverage tracks files (bigWig) for the UCSC genome browser [8] were generated considering just reads with a unique mapping position on the genome, those reads were fished out from the bam files using the option *-q 1* of SAM tools [9]. Profile were obtained using *genomeCoverageBed* from Bed Tools v2.17.0 and then linearly re-scaled according to sequencing depth (RPM, Reads Per Million sequenced reads [10]. Reads quantification was calculated using the *featureCount* function of the Subread package [11]. *edger* was used to assess differential expression [12]. Libraries were normalized according to TMM normalization. Differentially expressed genes (DEGs) were defined as those showing a

FDR ≤0.05 and a linear fold-change ≥1.5. R was used to run *edger* and to generate the heatmaps and plots. Functional annotation and enrichment of differentially expressed genes (DEGs) were analyzed through the use of Ingenuity Pathway Analysis (IPA;QIAGENInc.) at(https://www.qiagenbioinformatics.com/products/ingenuitypathway-analysis). The datasets generated in this study have been deposited in NCBI's Gene Expression Omnibus and are accessible through GEO Series accession number GSE125719 (https://www.ncbi.nlm.nih.gov/geo/query/acc.cgi?acc=GSE125719).

Chromatin immunoprecipitation quantitative PCR (ChIP-qPCR)

Chromatin immunoprecipitation (ChIP) assays for LSD1, H3K4me2, H3K4me3, H3K9Ac, H3K27ac and IgG were performed after treating the cells as indicated. For LSD1 and histone marks immunoprecipitation, 200×10^6 and 5×10^6 human AML cells per immunoprecipitation were used respectively. Briefly, after crosslinking with 1% paraformaldehyde for 10 min and quenching with 0.125M glycine for 5 min, cells were washed twice with ice-cold PBS, lysed and resuspended in IP buffer and sonicated. Sonicated lysates were then precleared with BSA-blocked Protein A Sepharose beads. An aliquot was used as an input control, whereas the rest of the sonicated samples were incubated overnight at 4°C with the indicated antibodies and precipitated with 30 µl of Protein G Dynabeads. Following washing cycles, the precipitated magnetic beads were treated with elution buffer. Cross-links of the eluted samples were reversed by incubating them overnight at 65°C. After protein digestion with Proteinase K, DNA was eventually purified using a PCR Purification Kit (Qiagen) and analyzed by real-time qPCR.

Clonogenic assay

AML cells were treated as indicated and cultured in MethoCult H4435 Enriched (StemCell Technologies, Vancouver, BC) according to the manufacturer instructions for the indicated time point of treatment. Colonies were then counted and cytospin preparations of the obtained cells were then stained using May Grunwald Giemsa staining.

FACS analysis of infiltration of human AML cells

Peripheral blood samples were collected via tail bleeding. Spleen and femur bone marrow samples were also harvested two weeks after treatment. RBCs were lysed using RBC lysis buffer and the remaining mononucleated cells were pelleted by centrifugation. The pellet was washed once using ice-cold PBS. Cells were then stained with anti-human CD45 PerCP

diluted in 5% BSA in PBS at 4^{o}C for 30 min, washed in 1% BSA in PBS and fixed in formaldehyde (final concentration 1%) for 20 min on ice. Fixed cells were then washed in 1% BSA in PBS and resuspended in PBS. FACS acquisition was carried out using FACS Calibur and data were analyzed using FlowJo software.

Histopathological examination

Paraformaldehyde-fixed (4%) samples of murine spleen, bone marrow and muscle tissues were paraffin embedded using Diapath automatic processor. Haematoxylin and eosin (Diapath) staining was performed according to the standard protocol and samples were mounted in EuKitt (Bio-Optica). The degree of leukemia infiltration was scored by a pathologist blinded to the experimental groups.

Immunohistochemistry

For IHC analysis, paraffin was removed using xylene and sections were rehydrated in graded alcohol. Antigen retrieval was carried out using a preheated target retrieval solution for 45 min. Tissue sections were blocked using FBS in PBS for 60 min and incubated overnight with one of the following primary antibodies; anti-human nuclei antibody (1:200) to clearly identify/distinguish infiltrating primary human leukemic cells and anti-phospho-S6 ribosomal protein (1:300) as readout of mTOR activity. Antibody binding was detected using polymer detection kit (GAR-HRP and GAM-HRP, Microtech) followed by diaminobenzidine chromogen reaction (Peroxidase substrate kit, DAB, SK-4100; Vector Lab). All sections were counterstained with Mayer's hematoxylin and visualized using bright-field microscope.

Statistical analysis

Analysis of data was performed using GraphPad Instat (Version 2) as follows; data are presented as mean ± standard deviation (SD). Unless otherwise indicated, Student's t-test was used to compare two different treatment groups. Multiple comparisons for more than two treatment groups were carried out using either one way analysis of variance (ANOVA) followed by Dunett test for *post-hoc* analysis or two-way ANOVA followed by Bonferroni *post-hoc* test. Mantel-Cox test was used to analyze Kaplan-Meier survival curve results. Statistical significance was acceptable at P value less than 0.05. Graphs were presented using Graphpad Prism software program (Version 5).

Appendix Supplementary Tables

Table S1. Predicted upstream regulators obtained from IPA upstream analysis of KASUMI-1 cells 6h following their treatment with DDP38003 (0.5μM).

Upstream Regulator	Predicted Activation State	Activation z-score	P-value of overlap	Target molecules in dataset
DOCK8	Activated	2,000	1,60E-02	EDN1,LTA,RILPL1, TLR3
Ifnar	Activated	2,224	7,55E-03	CCL2,CD86,GBP2, OAS1,TLR3
IL4	Activated	2,975	1,93E-02	CD163,CD2,CNR2, CXCR3,GBP2,GZMA,IL 1RN,LRP1,LTA,PMP22, STAB1
CD44	Activated	2,414	1,38E-03	ACKR3,ADGRE1, CXCR3,IL1RN,SELL,TI AM1,TLR8
SAMSN1	Activated	2,000	3,52E-02	EDN1,LTA,RILPL1, TLR3
MET	Activated	2,000	6,44E-03	EDN1,LTA,RILPL1, TLR3
HNF1A	Activated	2,236	2,61E-02	DCT,EBF1,FFAR2, PRLR,RNASE4,TMPRS S4
SASH1	Activated	2,000	1,76E-02	EDN1,LTA,RILPL1, TLR3
IL6	Activated	2,200	2,68E-02	A2M,ADGRE1,CXCR3, HFE,IL1RN,ITGAM

Table S2.Predicted upstream regulators obtained from IPA upstream analysis of KASUMI-1 cells 72h following their treatment with DDP38003 (0.5µM).

Upstream Regulator	Predicted Activation State	Activation z-score	P-value of overlap	Target molecules in dataset
IL4	Activated	2,813	1,93E-02	CD163,CD2,CNR2, CXCR3,GBP2,GZMA, IL1RN,LRP1,LTA, PMP22,STAB1
CHUK	Activated	2,200	6,38E-03	ACKR3,GBP2,IL1A, IL1RN,TLR3,TMEM17 6B
CD44	Activated	2,414	1,38E-03	ACKR3,ADGRE1, CXCR3,IL1RN,SELL, TIAM1,TLR8
HNF1A	Activated	2,236	2,61E-02	DCT,EBF1,FFAR2, PRLR,RNASE4, TMPRSS4
IL6	Activated	2,200	2,68E-02	A2M,ADGRE1,CXCR3 ,HFE,IL1RN,ITGAM

Table S3. Predicted upstream regulators obtained from IPA upstream analysis of THP-1 cells 24h following their treatment with DDP38003 (0.5μM).

Upstream Regulator	Predicted Activation State	Activation z-score	P-value of overlap	Target molecules in dataset
Alpha catenin	Inhibited	-2,380	1,52E-04	FFAR2,GPR34, MPEG1, PLBD1
TRAF2	Inhibited	-2,000	7,34E-03	FFAR2,GPR34, MPEG1, PLBD1
TRAF3	Inhibited	-2,000	1,31E-02	CYBB,CYP19A1, IL1A, VCAN
ERK1/2	Activated	2,000	3,03E-02	IL15,LTA,RILPL1, TLR3
DOCK8	Activated	2,000	3,33E-02	CCL2,CD86,GBP2, IL15,OAS1,TLR3
Ifnar	Activated	2,434	4,34E-03	ITGAM,MYOG, S100A8,S100A9,TRIM63
TNFSF12	Activated	2,219	1,15E-02	CCL2,CD14,CD163, CD86,FCGR2B,GBP2,GPR34,IL15,IL1A, ITGAM,LTA,RILPL1,SLC6A12,TLR3, TRIM63
TLR4	Activated	2,438	1,19E-04	ADAM19,ANXA2, CD163,CD2,CLEC10A,CNR2,CXCR3, GBP2,GZMA,IL18R1,IL1RN,LRP1,LTA,P

				MP22,STAB1,VIM
IL4	Activated	2,554	1,27E-03	CRHBP,GPR65,IL1A, IL1RN,LY96,S100A9
mir-223	Activated	2,449	1,06E-02	ACKR3,ADGRE1, CXCR3,IL1RN,MOG AT1,SELL,TIAM1,T LR8
CD44	Activated	2,611	1,15E-03	IL15,LTA,RILPL1, TLR3
CRKL	Activated	2,000	1,10E-04	CCL2,CXCL14,EBF1 ,IL15,IL1A,LTA
CDKN2A	Activated	2,000	1,02E-02	IL15,LTA,RILPL1, TLR3
MET	Activated	2,000	1,40E-02	CCL2,CD86,FPR1, IL15,IL1A,TLR3
TICAM1	Activated	2,401	2,02E-02	BLNK,CD86,ID3, PGR
SATB1	Activated	2,000	3,18E-02	CD86,IL1A,S100A8, S100A9
IL12B	Activated	2,000	4,76E-03	IL15,LTA,RILPL1, TLR3
SASH1	Activated	2,000	3,64E-02	CYP19A1,MYOG, TMEM176A,TMEM1 76B,VWF
LIF	Activated	2,236	1,21E-02	IL15,LTA,RILPL1, TLR3
ARHGAP 21	Activated	2,000	6,77E-03	BLNK,CD86,CLEC1 0A,CLEC4M,GEM

SPIB	Activated	2,213	1,28E-02	FFAR2,GPR34, MPEG1,PLBD1

Table S4. Predicted upstream regulators obtained from IPA upstream analysis of THP-1 cells 72h following their treatment with DDP38003 (0.5μM).

Upstream Regulator	Predicted Activation State	Activation z-score	P-value of overlap	Target molecules in dataset
Alpha catenin	Inhibited	-2,380	1,52E-04	ADAMTS12,ADAMTS5, CXCL12,FMNL2,ITGAM, LYZ,S100A8,S100A9,VIM
ERK1/2	Activated	2,000	3,03E-02	CYBB,CYP19A1,IL1A, VCAN
MGEA5	Activated	2,121	4,68E-03	ADAMTS5,CALCRL, CCL2,CD14,CD53,CD86, GP9,GPR34,IL21R
DOCK8	Activated	2,000	3,33E-02	IL15,LTA,RILPL1,TLR3
Ifnar	Activated	2,434	4,34E-03	CCL2,CD86,GBP2,IL15, OAS1,TLR3
TNFSF12	Activated	2,219	1,15E-02	ITGAM,MYOG,S100A8, S100A9,TRIM63
TLR4	Activated	2,948	1,19E-04	CCL2,CD14,CD163,CD86, FCGR2B,GBP2,GPR34, IL15, IL1A, ITGAM, LTA, RILPL1,SLC6A12,TLR3, TRIM63
IL4	Activated	3,065	1,27E-03	ADAM19,ANXA2,CD163, CD2,CLEC10A,CNR2,CX CR3,GBP2,GZMA,IL18R1, IL1RN,LRP1,LTA,PMP22, STAB1,VIM
mir-223	Activated	2,236	1,06E-02	CRHBP,GPR65,IL1A,

				IL1RN,LY96,S100A9
CD44	Activated	2,611	1,15E-03	ACKR3,ADGRE1,CXCR3, IL1RN,MOGAT1,SELL,TI AM1,TLR8
CRKL	Activated	2,000	1,10E-04	IL15,LTA,RILPL1,TLR3
CDKN2A	Activated	2,000	1,02E-02	CCL2,CXCL14,EBF1,IL15, IL1A,LTA
MET	Activated	2,000	1,40E-02	IL15,LTA,RILPL1,TLR3
TICAM1	Activated	2,401	2,02E-02	CCL2,CD86,FPR1,IL15, IL1A,TLR3
SATB1	Activated	2,000	3,18E-02	BLNK,CD86,ID3,PGR
IL12B	Activated	2,000	4,76E-03	CD86,IL1A,S100A8, S100A9
SASH1	Activated	2,000	3,64E-02	IL15,LTA,RILPL1,TLR3
LIF	Activated	2,236	1,21E-02	CYP19A1,MYOG,TMEM1 76A,TMEM176B,VWF
ARHGAP21	Activated	2,000	6,77E-03	IL15,LTA,RILPL1,TLR3
SPIB	Activated	2,213	1,28E-02	BLNK,CD86,CLEC10A, CLEC4M,GEM

Table S5. List of differentially expressed genes (DEGs) in THP-1 and KASUMI-1 cells following the indicated time points of treatment with DDP38003 (0.5μM).

KASUMI-1_6h N=175	KASUMI-1_24h N=192	THP-1_24h N=205	THP-1_72h N=196
A2M	A2M	ABCG2	ABCA6
ABI3	ABCA6	ACADL	ACOX2
ACADL	ABCG2	ACOX2	ACVR1C
ACVR1C	ABI3	ADAM19	ADAM19
ADAM28	ACVR1C	ADAM28	ADAM28
ADAP2	ADAM28	ADAMTS12	ADAMTS12
AMICA1	ADAMTS12	ADAMTS5	ADAMTS5
ASPN	AF064861.93	ADAP2	ADAP2
B3GALT2	AIM1	ADORA1	AIM1
BAI3	AKR1C4	AF064861.93	AKR1C4
BCL2L14	ALOX5	AIM1	ALDH7A1
BHLHE41	APOL3	AKR1C4	ALOX5
BX296545.5	ASB15	ALDH7A1	AMDHD1
C10orf67	ASPN	ALOX15	AMICA1
C11orf41	B3GALT2	ALOX5	ANXA2
C1orf62	BAI2	AMDHD1	APOA2
C1QTNF1	BAI3	AMICA1	APOL3
C20orf26	BHLHE41	ANXA2	ARL4C
C4orf18	BLNK	APOL3	ASB15
C4orf44	BX296545.5	BAI2	BAI2
CABP4	C10orf141	BIRC7	BIRC7
CALCB	C10orf67	BLNK	BLNK
CALCRL	C11orf41	BMX	BMX
CALHM3	C15orf53	BTBD11	C10orf67
CAMSAP1L1	C16orf45	C11orf41	C16orf45
CASP5	C17orf99	C16orf45	C1orf62
CCDC46	C1orf62	C1QL4	C1QL4
CCL2	C1QL4	C21orf93	C20orf26

CD163	C20orf26	C4orf44	C21orf93
CD1C	C4orf18	C7orf23	C4orf44
CD5	C7orf51	C7orf51	C7orf23
CD86	CABP4	C7orf58	C7orf51
CEACAM6	CACNA1G	CACNA2D1	C7orf58
CFH	CACNA2D1	CADM1	CACNA1G
CLUL1	CALCB	CALCB	CADM1
CMKLR1	CALCRL	CAMK2A	CALCRL
CNR2	CALHM3	CASP5	CALHM3
CRHBP	CAMK2A	CBLN1	CASP5
CSAG2	CAMSAP1L1	CCDC109B	CCDC109B
CXCL11	CCDC46	CCDC129	CCDC46
CXCL14	CD14	CCDC46	CCL13
CXCL5	CD163	CCL2	CCL2
CXCR3	CD2	CD14	CD14
CXCR7	CD3E	CD163	CD163
CYP2C18	CD5	CD1A	CD1C
DCT	CD86	CD1B	CD2
DDX43	CFH	CD1C	CD5
ECM2	CHN2	CD1E	CD53
EDN1	CHRNA6	CD2	CD86
EPB41L3	CLEC12A	CD5	CEACAM6
EPN3	CLEC4A	CD53	CFH
ETV1	CNR2	CD86	CHN2
F9	COL28A1	CEACAM6	CHRNA6
FAIM3	COLEC12	CFH	CLEC12A
FAM108A6	CRHBP	CHN2	CLEC4A
FAM162B	CSAG2	CHRNA6	CLUL1
FCRLA	CTTNBP2	CLEC4A	CNR2
FFAR2	CXCL14	CLUL1	COL28A1
FGD6	CXCL5	CNR2	CPT1C
FRG2B	CXCR7	CPT1C	CSPG2

GABRA4	CYP26B1	CRHBP	CXCL11
GCNT1P	CYP2C18	CSAG2	CXCL14
GEM	DCT	CSPG2	CXCR7
GIMAP4	DDIT4L	CXCL11	CYBB
GLIPR1	DDX43	CXCR3	CYP19A1
GNGT2	DES	CXCR7	DDIT4L
GPR143	DMD	CYBB	DMD
GPR15	DMGDH	DDIT4L	DSG2
GPR174	DSG2	DDX43	DTX4
GPR177	EBF1	DMD	EBF1
GPR183	ECM2	DOCK4	ECM2
GPR65	EDN1	DTX4	EMR1
GPR84	EGFLAM	EBF1	EPB41L3
GRIA3	EMR1	ENPP1	EPHB3
GZMA	ENPP1	EPB41L3	EPN3
HFE	EPHB3	EPHB3	ETV1
HORMAD1	EPN3	ETV1	EVPL
HPGD	ETV1	EVPL	FAIM3
ID3	F9	FAIM3	FAM162B
IGKC	FAIM3	FAM162B	FAM65B
IGSF3	FCGBP	FAM65B	FAP
IL1RN	FCGR2B	FAP	FCAMR
IL24	FCRLA	FCAMR	FCGBP
IL28B	FFAR2	FCGR2B	FCGR2B
IL31RA	FGD6	FCRLA	FCRLA
KCTD12	FPR1	FFAR2	FFAR2
KIAA1644	FRG2B	FGD2	FGD2
KISS1R	GABBR2	FMNL2	FGD6
KLF4	GABRA4	FPR1	FMNL2
KLHL34	GATA1	GABRA4	FPR1
LAMB4	GBP2	GABRD	GABRA4
LGALS2	GEM	GALR2	GABRD

LRFN5	GIMAP4	GBP2	GALR2
LRRC66	GLIPR1	GCNT1P	GBP2
LTA	GLYATL2	GCNT2	GCNT2
LY96	GNGT2	GEM	GIMAP4
LYZ	GP9	GIMAP4	GLIPR1
MAOA	GPR174	GLIPR1	GNGT2
MICF	GPR177	GPR143	GP9
MPEG1	GPR183	GPR177	GPR143
MS4A4A	GPR34	GPR34	GPR177
MS4A4E	GPR65	GPR65	GPR183
MTUS1	GPR84	GPR84	GPR65
NLRP1	GRAMD1C	GRAP2	GPR84
OMD	GRAP2	GRIA3	GRAMD1C
OR1L8	GZMA	GZMA	GRAP2
OR2L1P	HFE	HERC5	GZMA
OSBPL11	HLA-DMB	HFE	HERC5
P2RX6	IGKC	HLA-DMB	HFE
P2RX7	IGSF3	HORMAD1	HLA-DMB
P2RY5	IL1RN	HSPA6	HSPA6
PGLYRP3	IL31RA	ID3	ID3
PGLYRP4	ITGAM	IGSF6	IGKC
PHOSPHO1	JHDM1D	IL15	IGSF6
PI16	JSRP1	IL18R1	IL15
PITPNM3	KCNK13	IL1RN	IL18R1
PLN	KCTD12	IL24	IL1RN
PLVAP	KIF13A	IL28B	IL21R
PMP22	KISS1R	IL31RA	IL24
PRG4	KLF4	IRS1	IRS1
PRL	KLHL10	ITGAM	ITGAM
PRLR	LGSN	JHDM1D	JHDM1D
PRSS35	LPAR3	KCNK13	KCNK13
PSD	LPXN	KIAA1244	KCTD12

RAB17	LRFN5	KIF13A	KIAA1244
RASGEF1B	LRP1	KISS1R	KIAA1644
RGMB	LRRC66	KLF4	KIF13A
RIN2	LY96	KLHL10	KLHL10
RNASE1	LYZ	LILRB1	KLHL34
RNASE4	MAB21L2	LPAR3	LGSN
RNASE6	MAOA	LPAR3	LILRB1
RNF126P1	MBNL2	LPXN	LPXN
RPL8P2	MICF	LRFN5	LRFN5
RPS27AP7	MS4A4A	LRP1	LRP1
S100A12	MS4A4E	LRRC66	LRRC66
S100A5	MTUS1	LY96	LTA
S1PR1	MYO1A	LYZ	LY96
SEL1L2	NAGS	MBNL2	LYZ
SGMS2	NLRP1	METTL7A	MBNL2
SGSH	OAS1	MPZL1	METTL7A
SHH	OR1L8	MS4A4A	MPZL1
SHROOM3	OR2L1P	MYO1A	MS4A4A
SIRPB2	OSBPL11	NAGS	MTUS1
SLC1A3	P2RX7	NLRC4	MYO1A
SLC26A11	P2RY5	NLRP1	NAGS
SLC35D3	PCDHA1	OLFML3	NLRC4
SLC7A7	PGLYRP3	OMD	NLRP1
SLC7A8	PGLYRP4	OSBPL11	OAS1
SMARCA1	PI16	P2RX7	OLFML3
SNCAIP	PLBD1	PCDH7	OMD
SNX7	PLVAP	PDPN	OSBPL11
SP140	PMP22	PGLYRP4	P2RX7
ST6GALNAC5	PPP1R1C	PHOSPHO1	PCDH7
ST8SIA1	PRG4	PIGR	PCDHA1
SULF2	PRLR	PITPNM3	PDPN
TAS2R42	PRSS35	PLBD1	PGLYRP4

TEAD3	PSD	PLEKHC1	PHOSPHO1
TGM7	RAB17	PLVAP	PIGR
TLR1	RASGEF1B	PMP22	PLBD1
TLR3	RGMB	PPP1R1C	PLEKHC1
TLR8	RILPL1	PRG4	PRKAR2B
TMEM176A	RNASE4	PRKAR2B	PRL
TMEM176B	RPS27AP7	PRL	PRLR
TMEM178	S1PR1	PRLR	RASGEF1B
TMPRSS4	SDS	RAB17	RBM47
TNFAIP8L3	SEL1L2	RBM47	RGMB
TRAT1	SELL	RGMB	RIN2
TRIM2	SLC1A3	RILPL1	RNASE6
U66059.1-2	SLC7A7	RIN2	SDS
VIT	SMARCA1	RNASE6	SEL1L2
VWF	SMTNL1	RNF126P1	SELL
Z82248.1	SNAI2	RPS27AP7	SLC26A11
Z85996.1-2	SNCAIP	SEL1L2	SLC37A2
ZDHHC15	SNX7	SELL	SLC7A7
ZNF366	SP140	SEPT10	SLC7A8
	ST8SIA1	SEPT10	SMARCA1
	STAB1	SLC15A3	SNAI2
	SULF2	SLC1A3	SNX7
	SYN3	SLC26A11	SP140
	TLE2	SLC37A2	ST8SIA1
	TLR3	SLC7A7	STAB1
	TLR5	SLC7A8	SYN3
	TLR8	SLFN5	TBC1D4
	TMEM176A	SMARCA1	TDRD9
	TMPRSS4	SNAI2	TIMP3
	TRAT1	SNX7	TLE2
	TRIM2	SP140	TLR3
	TRIM22	SULF2	TLR5

	U66059.1-2	SYN3	TLR8
	YPEL4	TBC1D4	TMEM176A
	ZCCHC24	TDRD9	TRIM22
	ZDHHC15	TLE2	TRPM1
		TLR3	VIM
		TLR8	VIT
		TMEM176A	YPEL4
		TRIM2	ZNF366
		TRIM22	
		TRPM1	
		VIM	
		VIT	
		VWF	
		ZDHHC15	
		ZFPM2	
		ZFPM2	
		ZNF366	

Table S6. Oligonucleotide sequences of the small hairpin RNAs (shRNAs) used to knock down LSD1.

Target of shRNAs	Oligos sequence
Scramble shRNAs	AGTACGCGAAGAATACTATCGA
shRNAs against LSD1 #1	AAGTGATACTGTGCTTGTCCAC
shRNAs against LSD1 #2	ATCTCAGAAGATGAGTATTATT

Table S7. Sequences of primers used for RT-qPCR.

Primer	Primers' sequence
LSD1	F:AGACGACAGTTCTGGAGGGTA R: TCTTGAGAAGTCATCCGGTCA
CD11b	F: AACCCCTGGTTCACCTCCT R: CATGACATAAGGTCAAGGCTGT
GAPDH	F: TTCGCTCTCTGCTCCTCCTG R: CCTAGCCTCCCGGGTTTCTC

Table S8. Sequences of IRS1 primers used for ChIP-qPCR.

Primer	Primers' sequence
A	F: AGGCCAAAACCCTACTGTGC R: AGCTGGCACCATCCTTGTTT
B	F: GGTAAGACTGACCCACGGGA R: GATCCCCTCACCATGGCCTA
C	F:GAGGCTCCGAAAAACAACCG R:CGTGGATTTCAGAGTCGGGG
D	F: ATCAGTGACCGGCAAGGAAA R: CTGGAAGGACAGCCTCGAAA

References:

1. Vianello P, Botrugno OA, Cappa A, et al. Discovery of a Novel Inhibitor of Histone Lysine-Speci fi c Demethylase 1A (KDM1A/LSD1) as Orally Active Antitumor Agent. J Med Chem 2016; 59(4):1501–1517.

2. Binda C, Valente S, Romanenghi M, et al. Biochemical , Structural , and Biological Evaluation of Tranylcypromine Derivatives as Inhibitors of Histone Demethylases LSD1 and LSD2. J AM CHEM SOC 2010; 132(19):6827–6833.

3. Zhang X, Yashiro M, Qiu H. Establishment and Characterization of Multidrug-resistant Gastric Cancer Cell Lines. Anticancer Res 2010; 30(3):915–921.

4. Abdel-Aziz AK, Shouman S, El-Demerdash E, Elgendy M, Abdel-Naim AB. Chloroquine synergizes sunitinib cytotoxicity via modulating autophagic, apoptotic and angiogenic machineries. Chem Biol Interact 2014; 217:28–40.

5. McGrath JP, Williamson KE, Balasubramanian S, et al. Pharmacological inhibition of the histone lysine demethylase KDM1A suppresses the growth of multiple acute myeloid leukemia subtypes. Cancer Res 2016; 76(7):1975–1988.

6. Abdel-Aziz AK, Azab SSE, Youssef SS, El-Sayed AM, El-Demerdash E, Shouman S. Modulation of imatinib cytotoxicity by selenite in HCT116 colorectal cancer cells. Basic Clin Pharmacol Toxicol 2015; 116(1):37-46.

7. Kim D, Pertea G, Trapnell C, Pimentel H, Kelley R SS. TopHat2 : accurate alignment of transcriptomes in the presence of insertions, deletions and gene fusions. Genome Biol 2013; 14(4):R36:0–9.

8. Fujita PA, Rhead B, Zweig AS, et al. The UCSC genome browser database: Update 2011. Nucleic Acids Res 2011; 39:876–882.

9. Li H, Handsaker B, Wysoker A, et al. The Sequence Alignment/Map format and SAMtools. Bioinformatics 2009; 25(16):2078–2079.

10. Quinlan AR, Hall IM. BEDTools: A flexible suite of utilities for comparing genomic features. Bioinformatics 2010; 26(6):841–842.

11. Liao Y, Smyth GK, Shi W. FeatureCounts: An efficient general purpose program for assigning sequence reads to genomic features. Bioinformatics 2014; 30(7):923–930.

12. Robinson MD, McCarthy DJ, Smyth GK. edgeR: A Bioconductor package for differential expression analysis of digital gene expression data. Bioinformatics 2009; 26(1):139–140.

Fig.S1

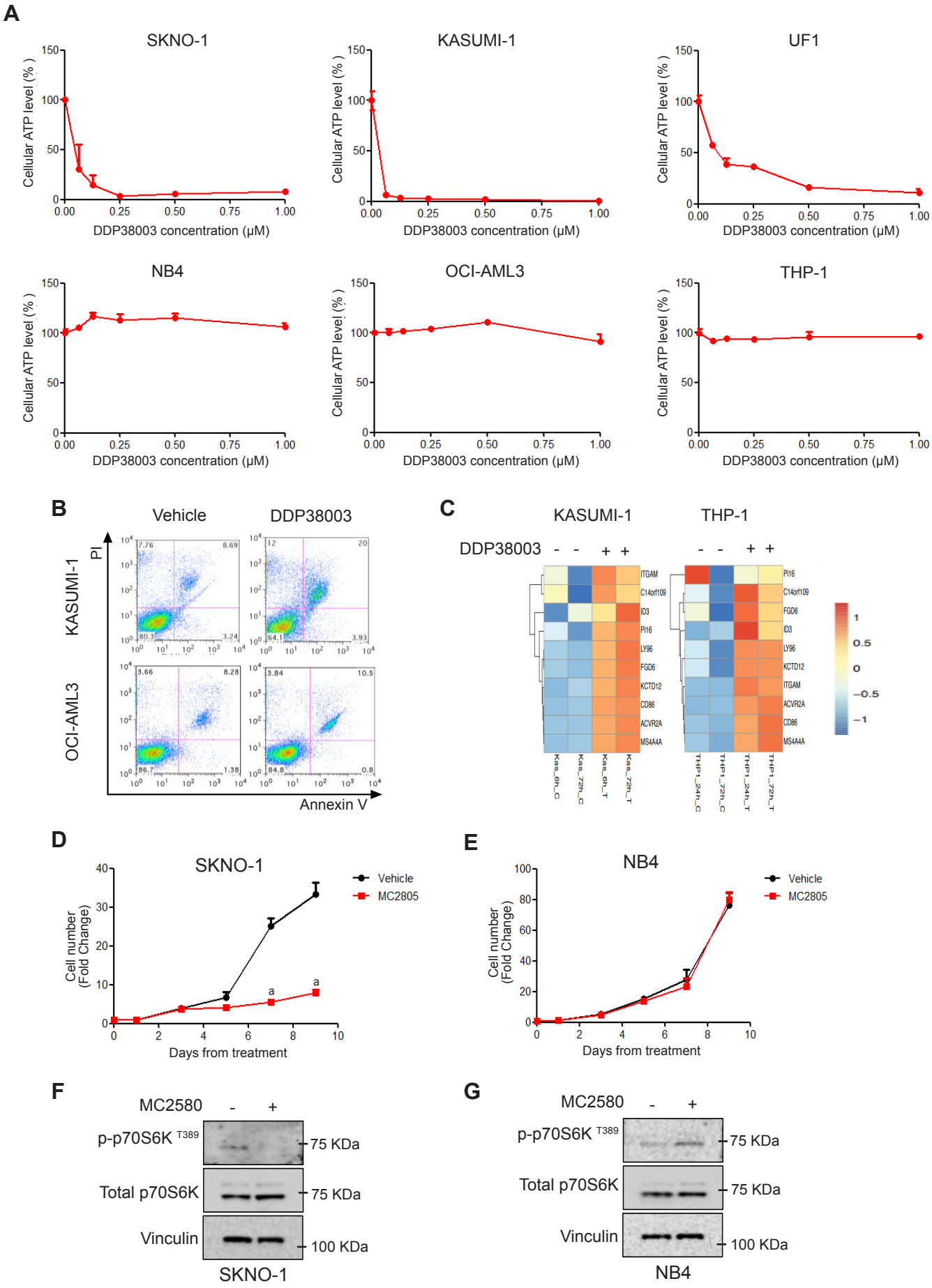
A
SKNO-1
KASUMI-1
UF1
NB4
OCI-AML3
THP-1
Cellular ATP level (%)
DDP38003 concentration (μM)
B
Vehicle
DDP38003
KASUMI-1
OCI-AML3
PI
Annexin V
C
KASUMI-1
THP-1
DDP38003
ITGAM
C14orf109
ID3
PI16
LY96
FGD6
KCTD12
CD86
ACVR2A
MS4A4A
D
SKNO-1
Vehicle
MC2805
Cell number (Fold Change)
Days from treatment
E
NB4
F
MC2580
p-p70S6K T389
Total p70S6K
Vinculin
75 KDa
100 KDa
SKNO-1
G
NB4

Fig.S2

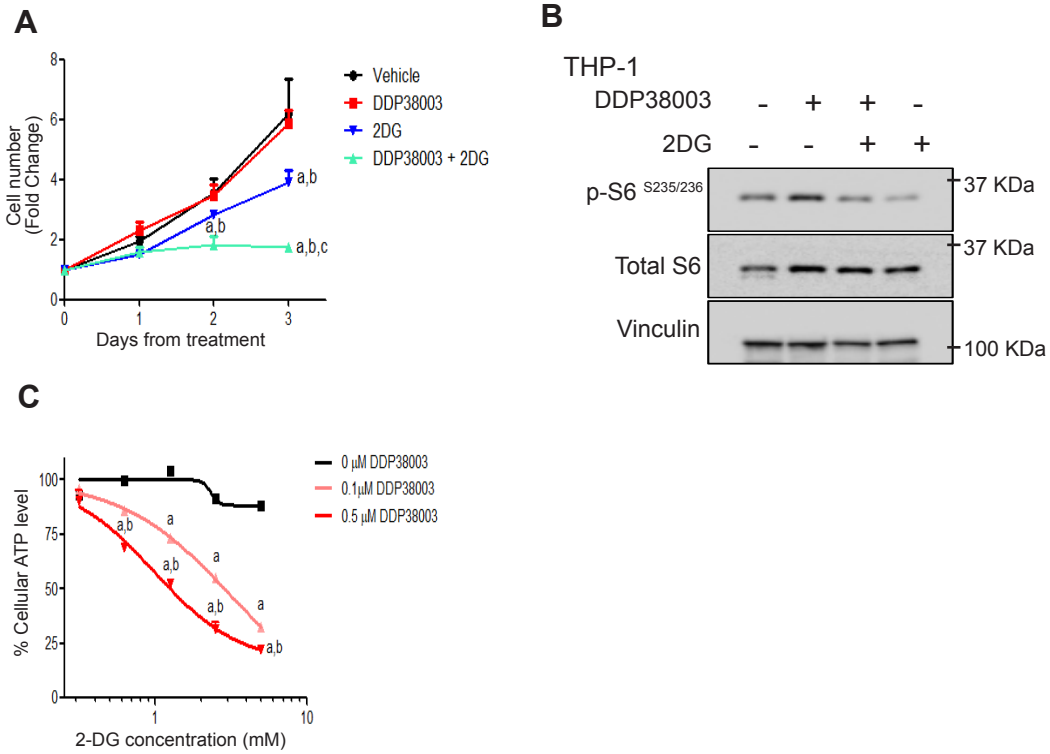
A
Cell number (Fold Change)
Days from treatment
Vehicle
DDP38003
2DG
DDP38003 + 2DG
a,b
a,b
a,b,c
B
THP-1
DDP38003 - + + -
2DG - - + +
p-S6 S235/236
Total S6
Vinculin
37 KDa
37 KDa
100 KDa
C
% Cellular ATP level
2-DG concentration (mM)
0 μM DDP38003
0.1μM DDP38003
0.5 μM DDP38003

Fig.S3

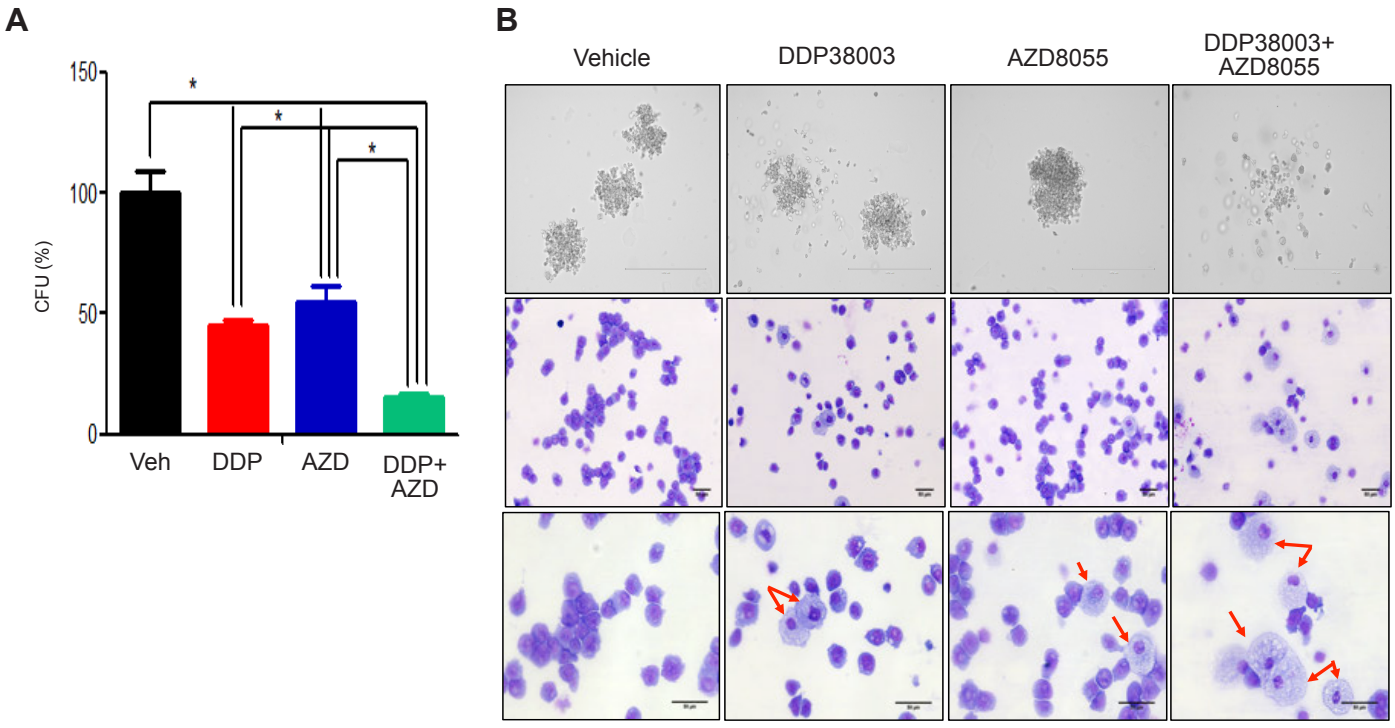
A
150
100
50
0
CFU (%)
*
*
*
Veh
DDP
AZD
DDP+
AZD
B
Vehicle
DDP38003
AZD8055
DDP38003+
AZD8055

Fig.S4

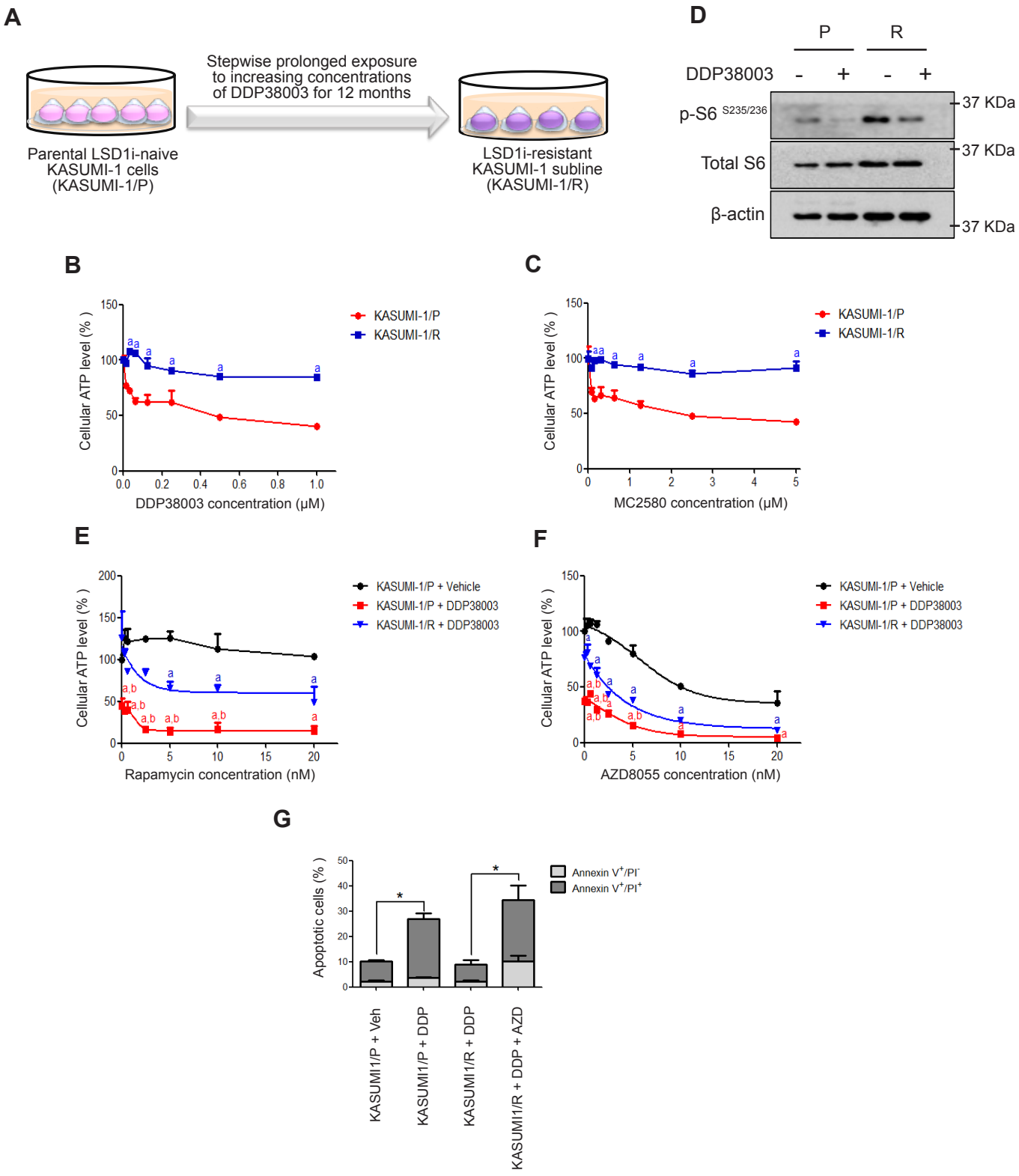
A
Stepwise prolonged exposure to increasing concentrations of DDP38003 for 12 months
Parental LSD1i-naive KASUMI-1 cells (KASUMI-1/P)
LSD1i-resistant KASUMI-1 subline (KASUMI-1/R)
D
P
R
DDP38003 - + - +
p-S6 S235/236
Total S6
β-actin
37 KDa
37 KDa
37 KDa
B
Cellular ATP level (%)
DDP38003 concentration (μM)
KASUMI-1/P
KASUMI-1/R
C
Cellular ATP level (%)
MC2580 concentration (μM)
KASUMI-1/P
KASUMI-1/R
E
Cellular ATP level (%)
Rapamycin concentration (nM)
KASUMI-1/P + Vehicle
KASUMI-1/P + DDP38003
KASUMI-1/R + DDP38003
F
Cellular ATP level (%)
AZD8055 concentration (nM)
KASUMI-1/P + Vehicle
KASUMI-1/P + DDP38003
KASUMI-1/R + DDP38003
G
Apoptotic cells (%)
Annexin V+/PI-
Annexin V+/PI+
KASUMI1/P + Veh
KASUMI1/P + DDP
KASUMI1/R + DDP
KASUMI1/R + DDP + AZD

Fig.S5

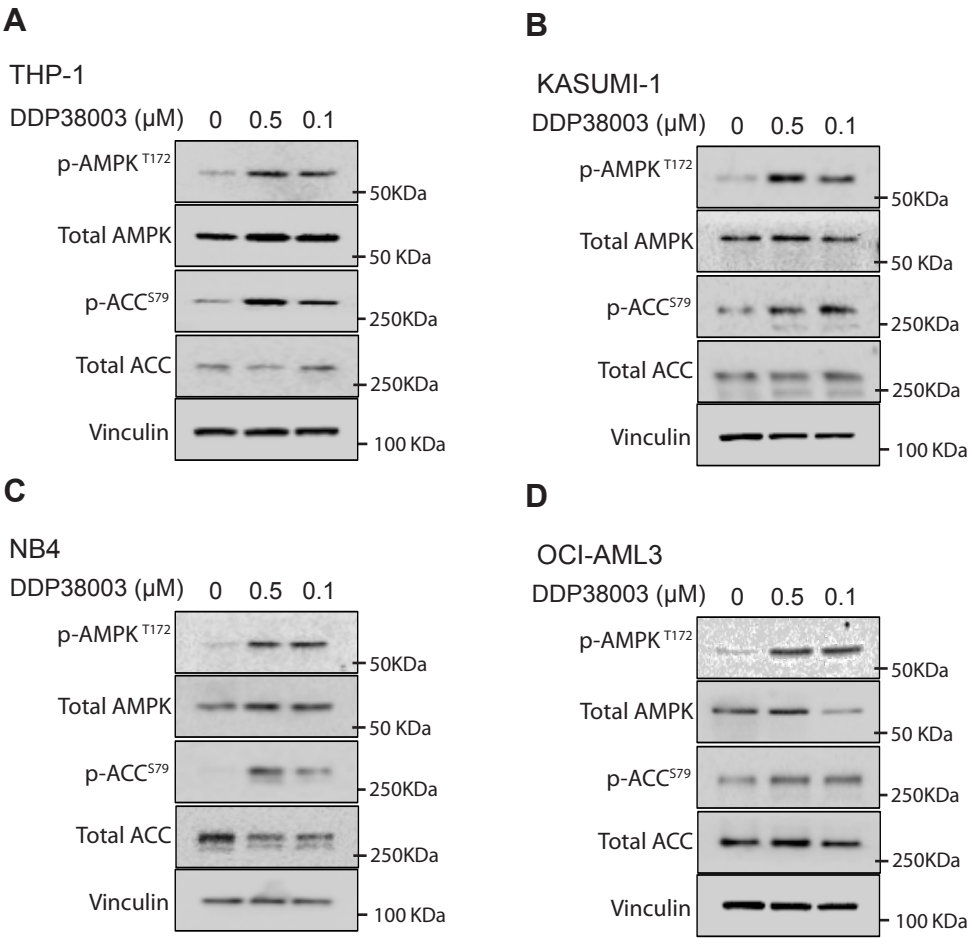
A
THP-1
DDP38003 (μM) 0 0.5 0.1
p-AMPK T172
Total AMPK
p-ACC S79
Total ACC
Vinculin
50KDa
50 KDa
250KDa
250KDa
100 KDa
B
KASUMI-1
DDP38003 (μM) 0 0.5 0.1
p-AMPK T172
Total AMPK
p-ACC S79
Total ACC
Vinculin
50KDa
50 KDa
250KDa
250KDa
100 KDa
C
NB4
DDP38003 (μM) 0 0.5 0.1
p-AMPK T172
Total AMPK
p-ACC S79
Total ACC
Vinculin
50KDa
50 KDa
250KDa
250KDa
100 KDa
D
OCI-AML3
DDP38003 (μM) 0 0.5 0.1
p-AMPK T172
Total AMPK
p-ACC S79
Total ACC
Vinculin
50KDa
50 KDa
250KDa
250KDa
100 KDa

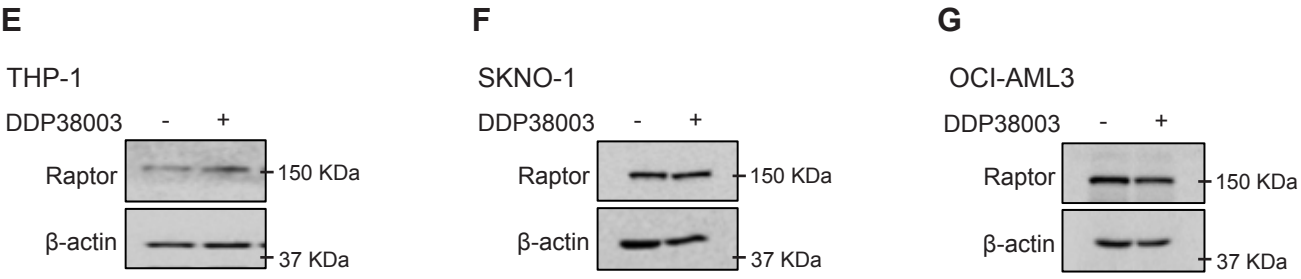
E
THP-1
DDP38003 - +
Raptor
β-actin
150 KDa
37 KDa
F
SKNO-1
DDP38003 - +
Raptor
β-actin
150 KDa
37 KDa
G
OCI-AML3
DDP38003 - +
Raptor
β-actin
150 KDa
37 KDa

Fig.S6

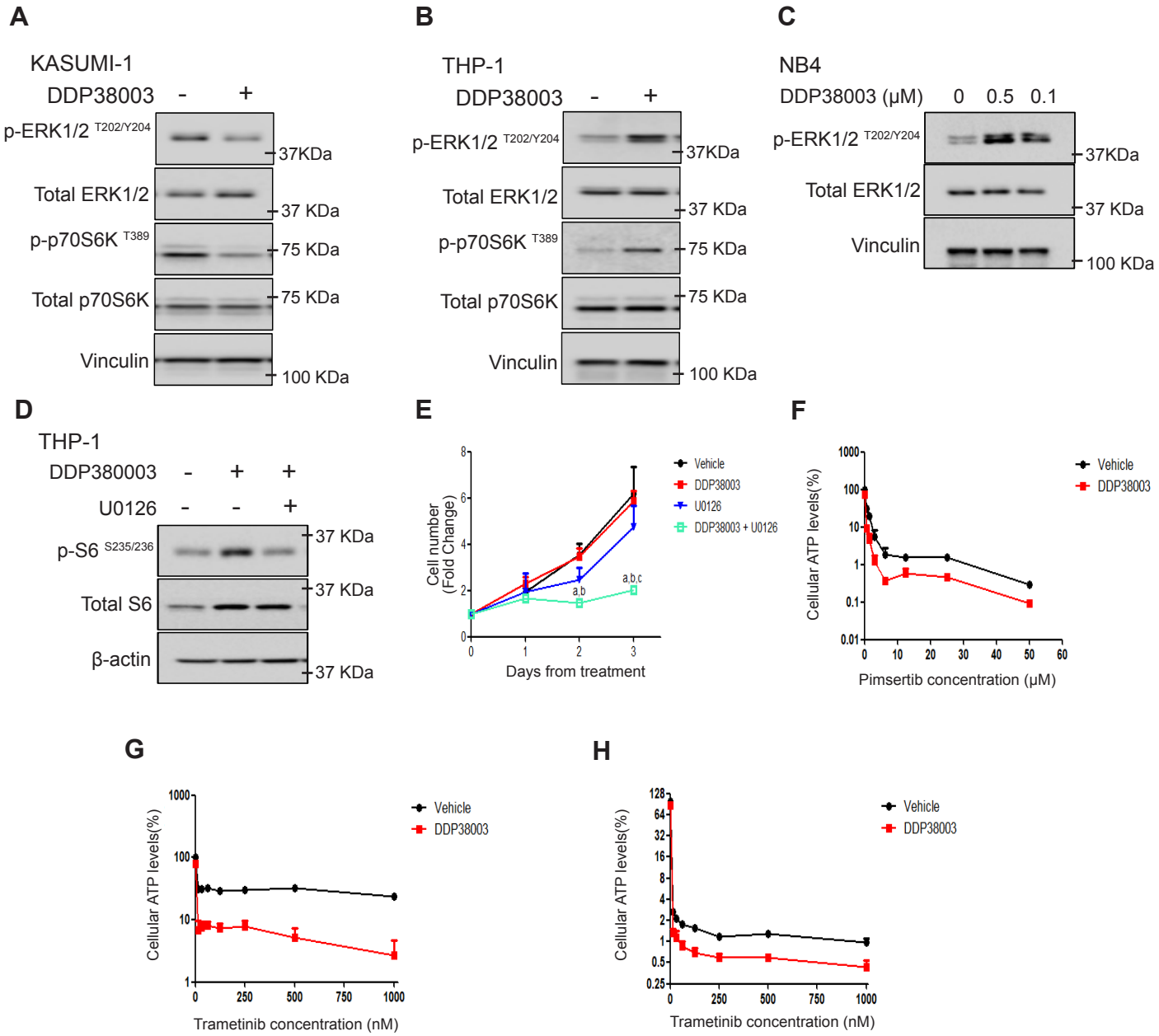
A
KASUMI-1
DDP38003 - +
p-ERK1/2 T202/Y204
37KDa
Total ERK1/2
37 KDa
p-p70S6K T389
75 KDa
Total p70S6K
75 KDa
Vinculin
100 KDa
B
THP-1
DDP38003 - +
p-ERK1/2 T202/Y204
37KDa
Total ERK1/2
37 KDa
p-p70S6K T389
75 KDa
Total p70S6K
75 KDa
Vinculin
100 KDa
C
NB4
DDP38003 (μM) 0 0.5 0.1
p-ERK1/2 T202/Y204
37KDa
Total ERK1/2
37 KDa
Vinculin
100 KDa
D
THP-1
DDP380003 - + +
U0126 - - +
p-S6 S235/236
37 KDa
Total S6
37 KDa
β-actin
37 KDa
E
Cell number (Fold Change)
Days from treatment
Vehicle
DDP38003
U0126
DDP38003 + U0126
a,b
a,b,c
F
Cellular ATP levels(%)
Pimsertib concentration (μM)
Vehicle
DDP38003
G
Cellular ATP levels(%)
Trametinib concentration (nM)
Vehicle
DDP38003
H
Cellular ATP levels(%)
Trametinib concentration (nM)
Vehicle
DDP38003

Fig.S7

A

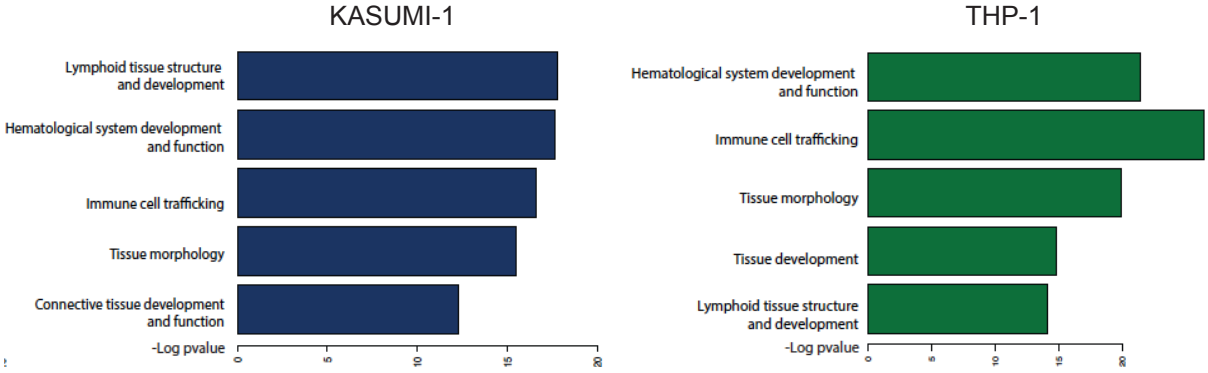
PHYSIOLOGICAL SYSTEM DEVELOPMENT AND FUNCTION
KASUMI-1
Lymphoid tissue structure and development
Hematological system development and function
Immune cell trafficking
Tissue morphology
Connective tissue development and function
-Log pvalue
0
5
10
15
20
THP-1
Hematological system development and function
Immune cell trafficking
Tissue morphology
Tissue development
Lymphoid tissue structure and development
-Log pvalue
0
5
10
15
20

B

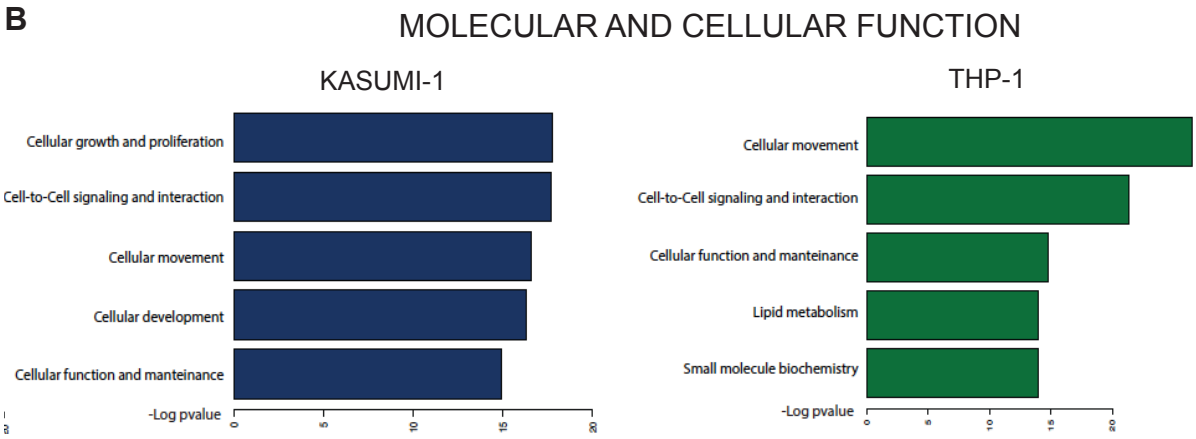
MOLECULAR AND CELLULAR FUNCTION
KASUMI-1
Cellular growth and proliferation
Cell-to-Cell signaling and interaction
Cellular movement
Cellular development
Cellular function and manteinance
-Log pvalue
0
5
10
15
20
THP-1
Cellular movement
Cell-to-Cell signaling and interaction
Cellular function and manteinance
Lipid metabolism
Small molecule biochemistry
-Log pvalue
0
5
10
15
20

Fig.S8

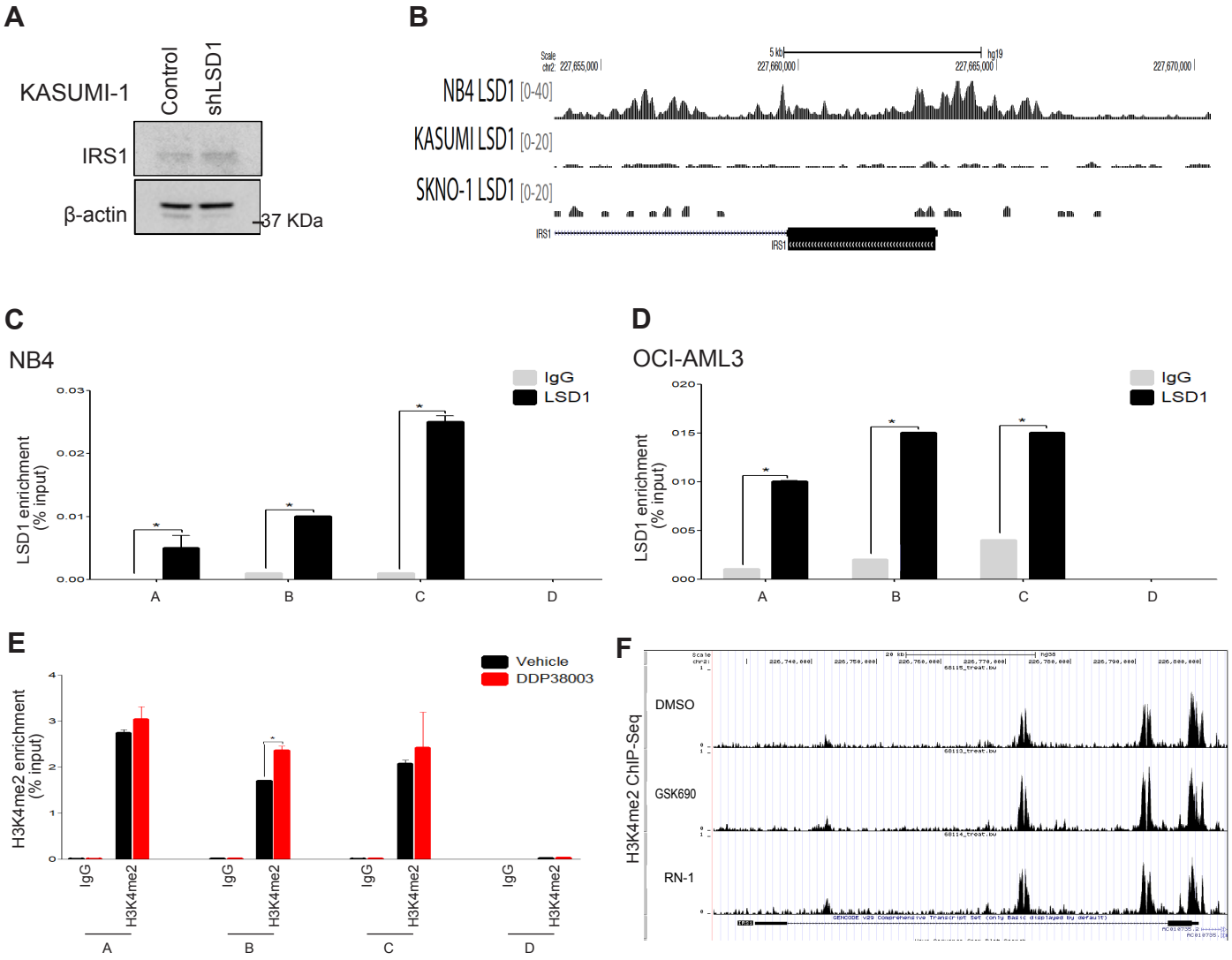
A
KASUMI-1
Control
shLSD1
IRS1
β-actin
37 KDa
B
NB4 LSD1 [0-40]
KASUMI LSD1 [0-20]
SKNO-1 LSD1 [0-20]
IRS1
C
NB4
IgG
LSD1
LSD1 enrichment (% input)
A
B
C
D
D
OCI-AML3
IgG
LSD1
LSD1 enrichment (% input)
A
B
C
D
E
Vehicle
DDP38003
H3K4me2 enrichment (% input)
IgG
H3K4me2
A
B
C
D
F
H3K4me2 ChIP-Seq
DMSO
GSK690
RN-1

Fig.S9

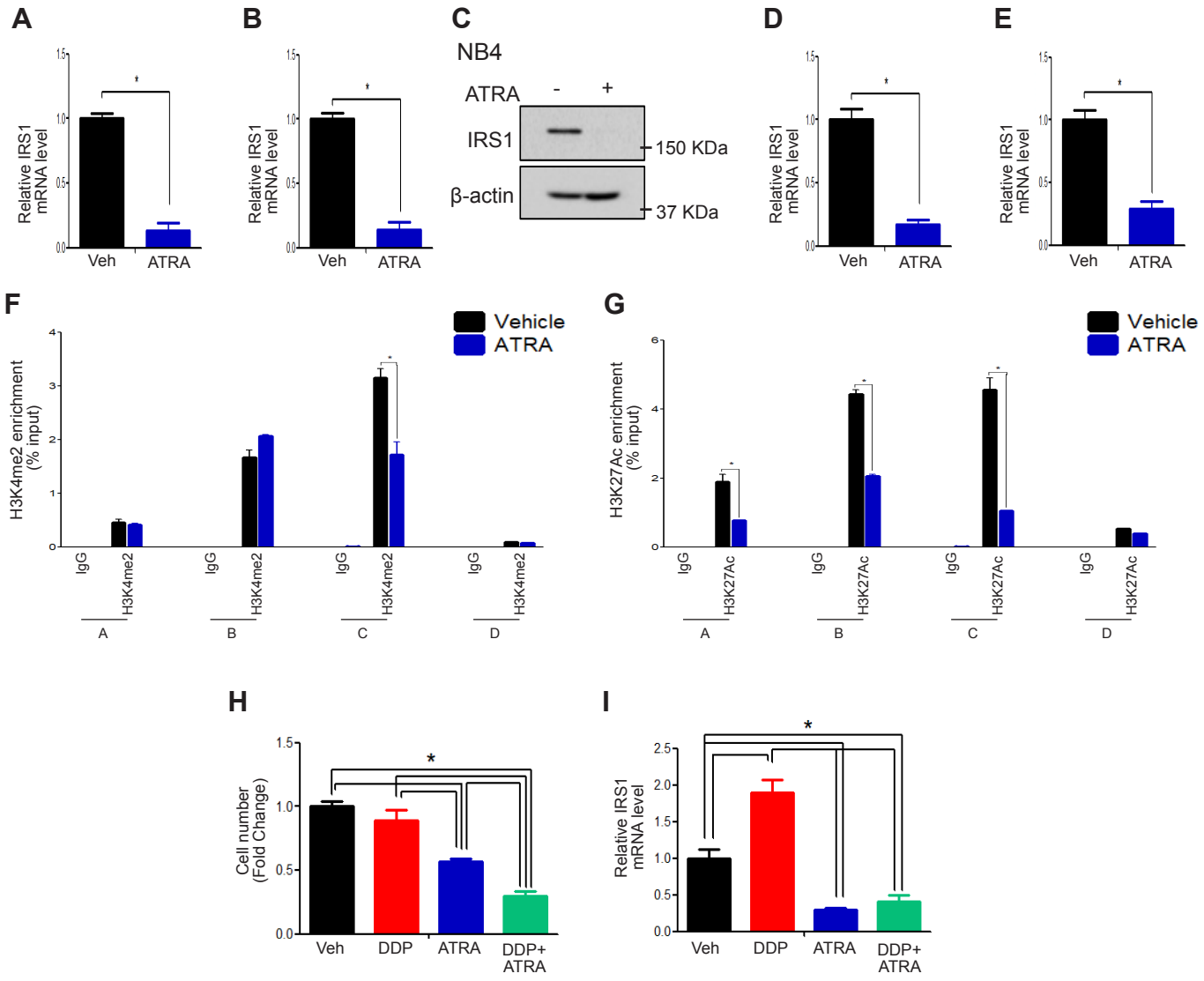
A
B
C
D
E
Relative IRS1 mRNA level
Veh
ATRA
NB4
ATRA
-
+
IRS1
β-actin
150 KDa
37 KDa
F
G
Vehicle
ATRA
H3K4me2 enrichment (% input)
H3K27Ac enrichment (% input)
IgG
H3K4me2
H3K27Ac
A
B
C
D
H
I
Cell number (Fold Change)
Veh
DDP
ATRA
DDP+ ATRA

Fig.S10

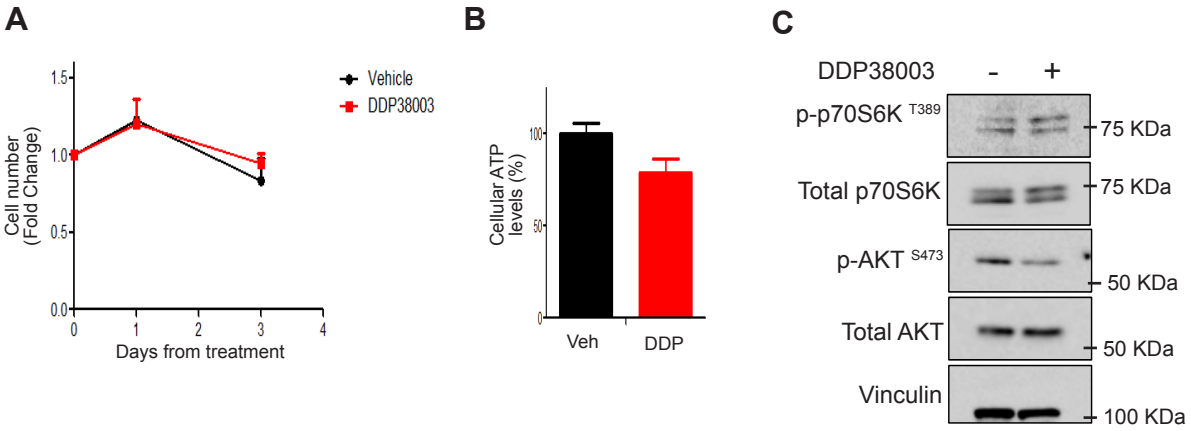
A
Vehicle
DDP38003
Cell number (Fold Change)
1.5
1.0
0.5
0.0
0
1
2
3
4
Days from treatment
B
Cellular ATP levels (%)
100
50
0
Veh
DDP
C
DDP38003
-
+
p-p70S6K T389
75 KDa
Total p70S6K
75 KDa
p-AKT S473
50 KDa
Total AKT
50 KDa
Vinculin
100 KDa

Fig.S11

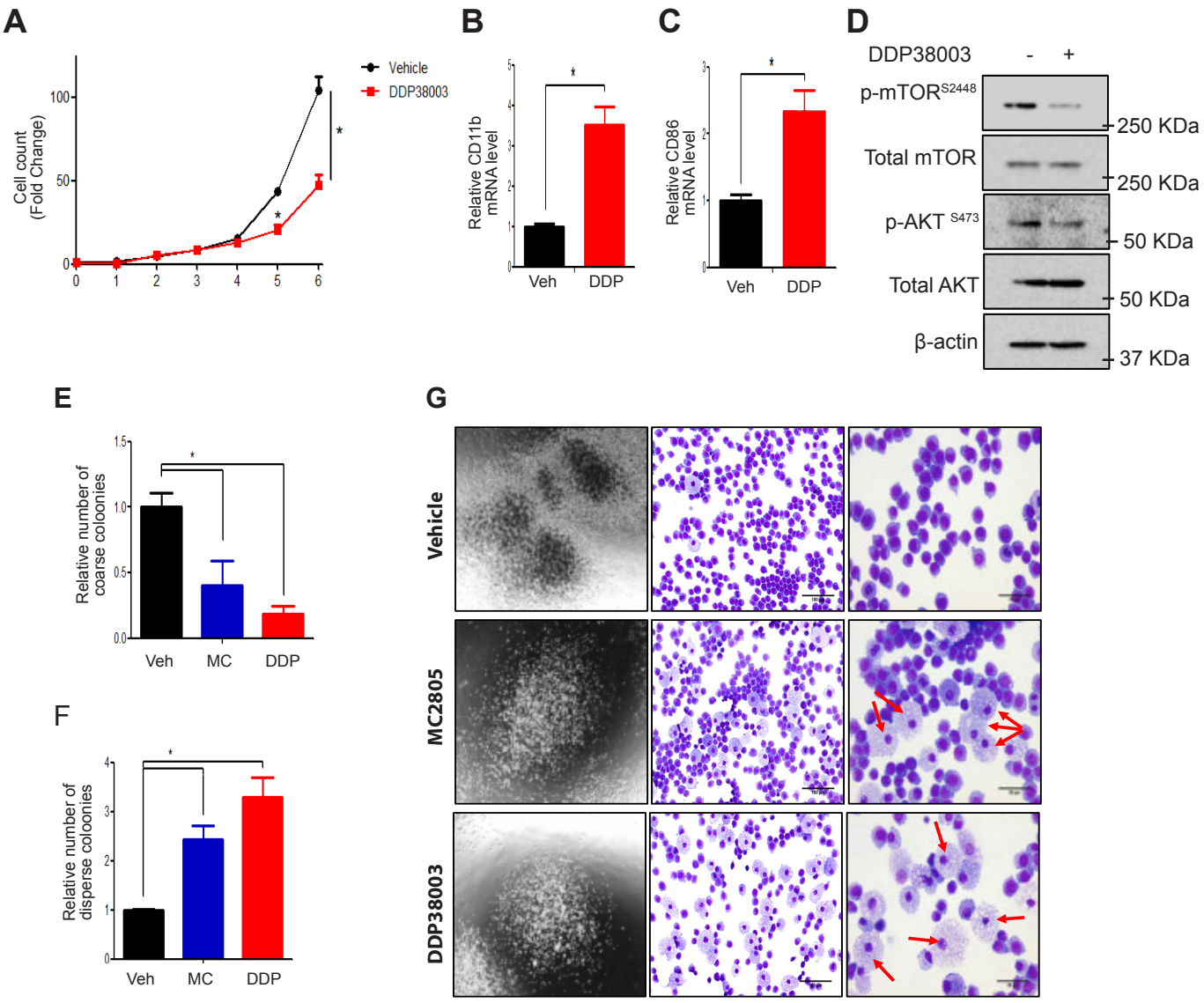
A
Cell count (Fold Change)
Vehicle
DDP38003
B
Relative CD11b mRNA level
Veh
DDP
C
Relative CD86 mRNA level
Veh
DDP
D
DDP38003 - +
p-mTOR S2448
Total mTOR
p-AKT S473
Total AKT
β-actin
250 KDa
250 KDa
50 KDa
50 KDa
37 KDa
E
Relative number of coarse coloonies
Veh
MC
DDP
F
Relative number of disperse coloonies
Veh
MC
DDP
G
Vehicle
MC2805
DDP38003

Fig.S12

A

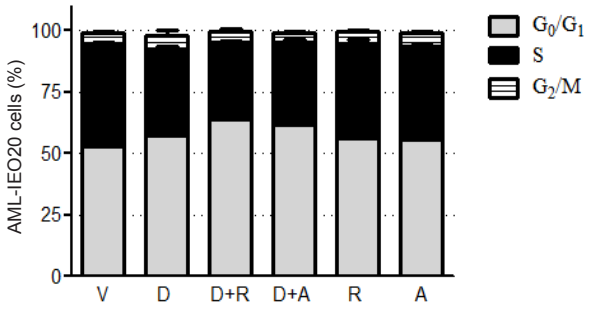
AML-IEO20 cells (%)
100
75
50
25
0
V
D
D+R
D+A
R
A
G0/G1
S
G2/M

B

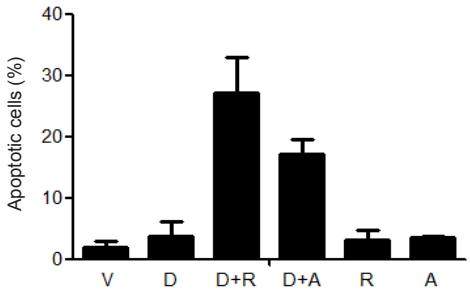
Apoptotic cells (%)
40
30
20
10
0
V
D
D+R
D+A
R
A

Fig.S12

C

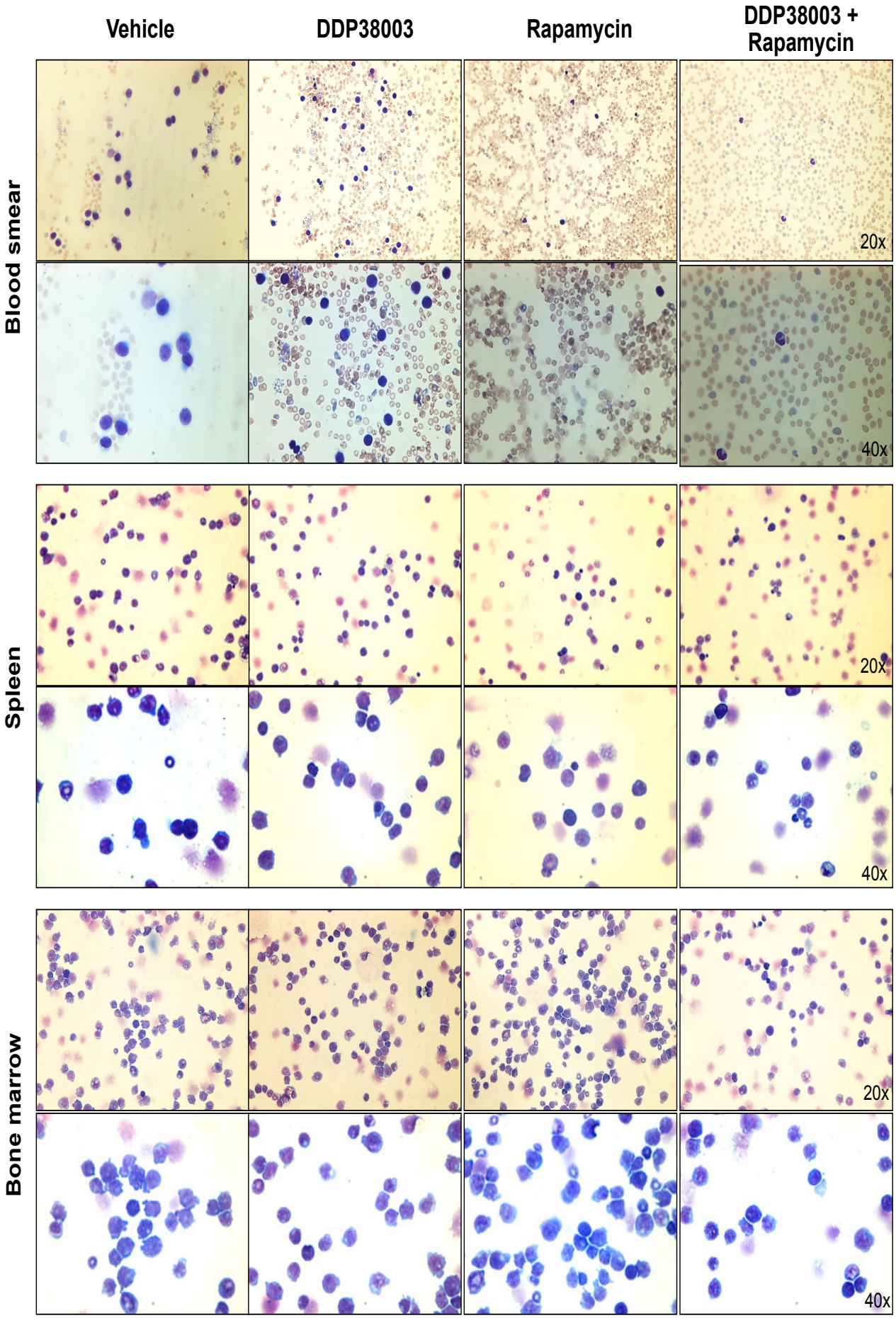
Vehicle
DDP38003
Rapamycin
DDP38003 + Rapamycin
Blood smear
Spleen
Bone marrow
20x
40x
20x
40x
20x
40x

Fig.S12

D

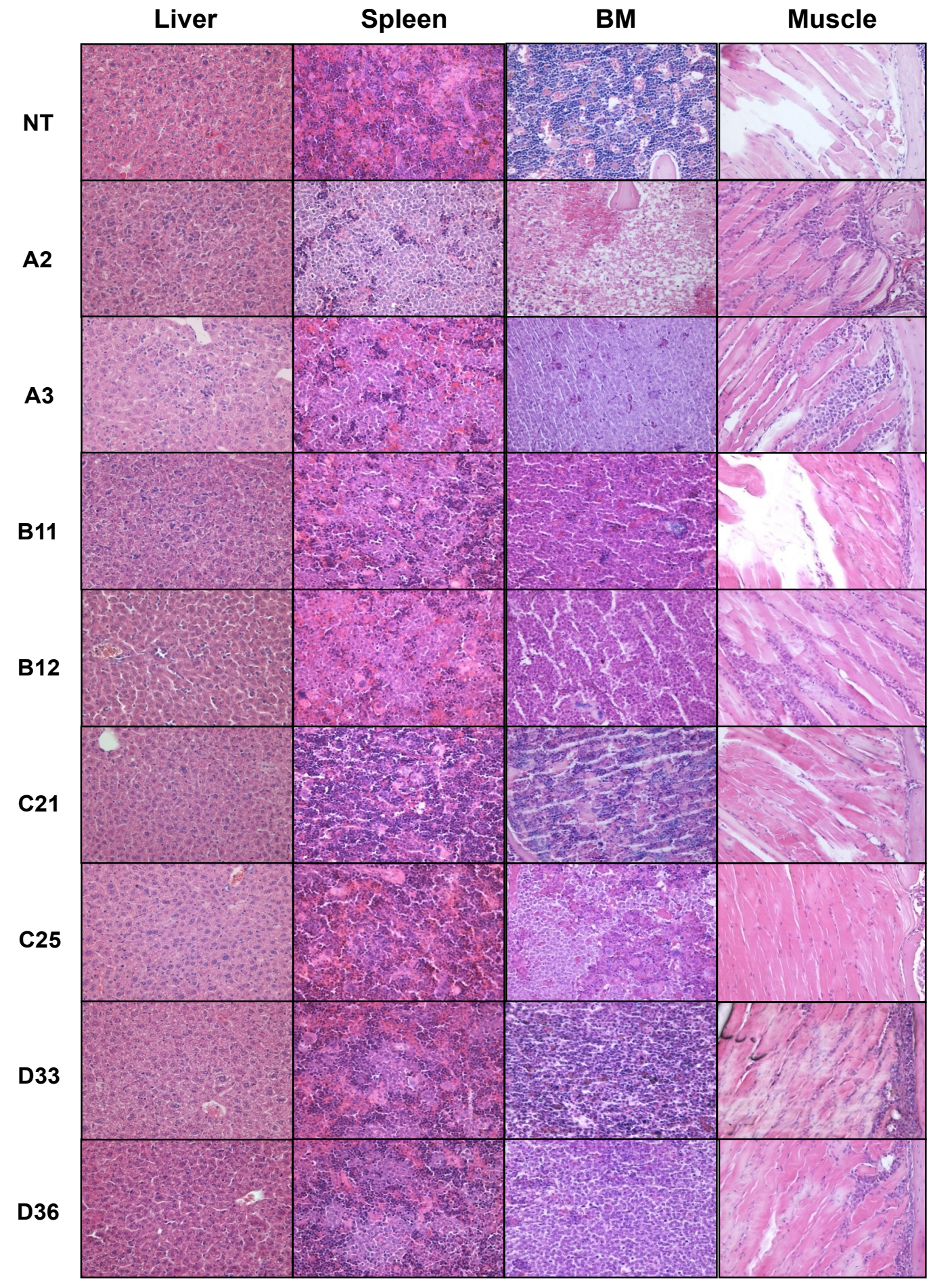

Fig.S12

E

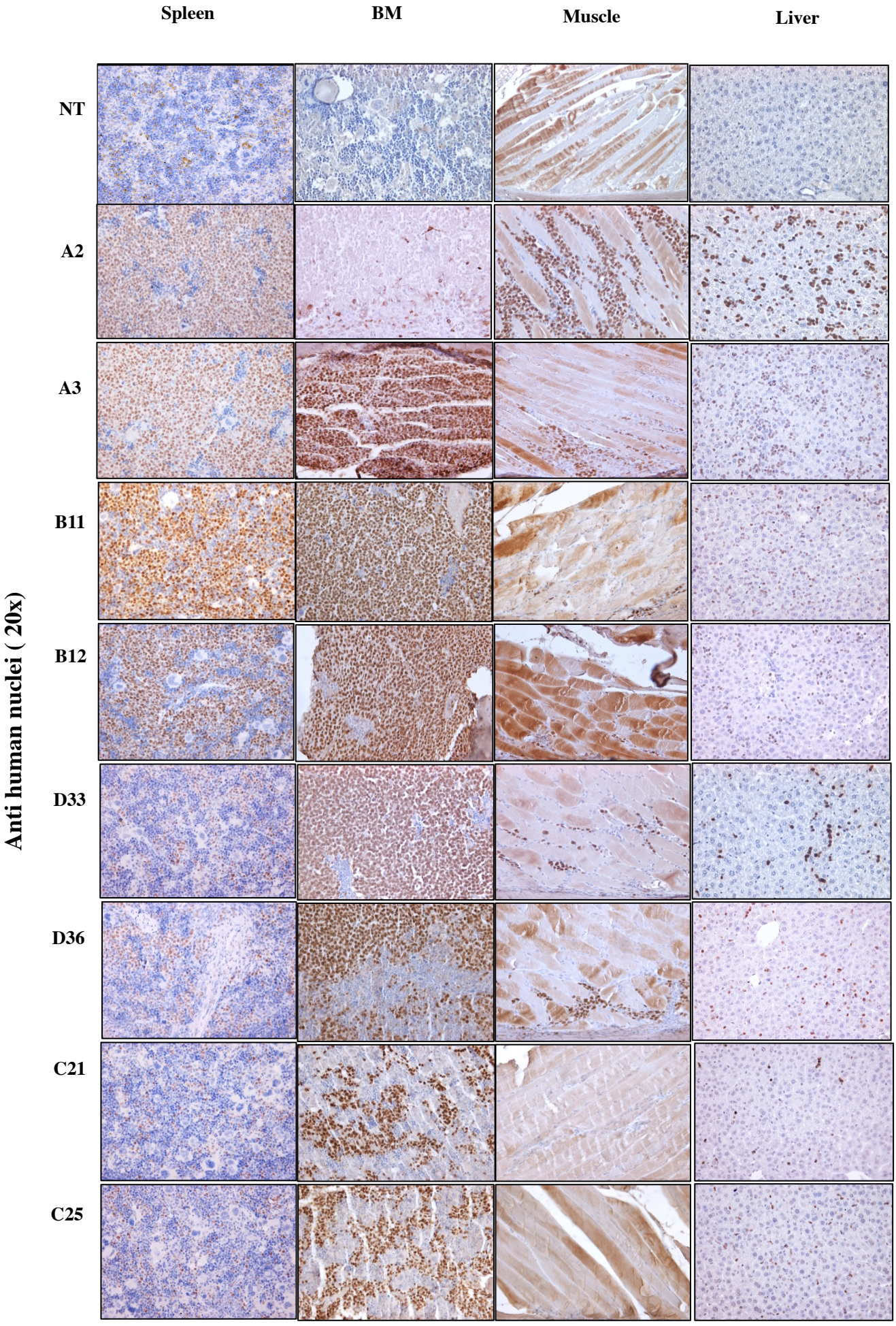
Spleen
BM
Muscle
Liver
NT
A2
A3
B11
B12
D33
D36
C21
C25
Anti human nuclei (20x)

Fig.S12

F

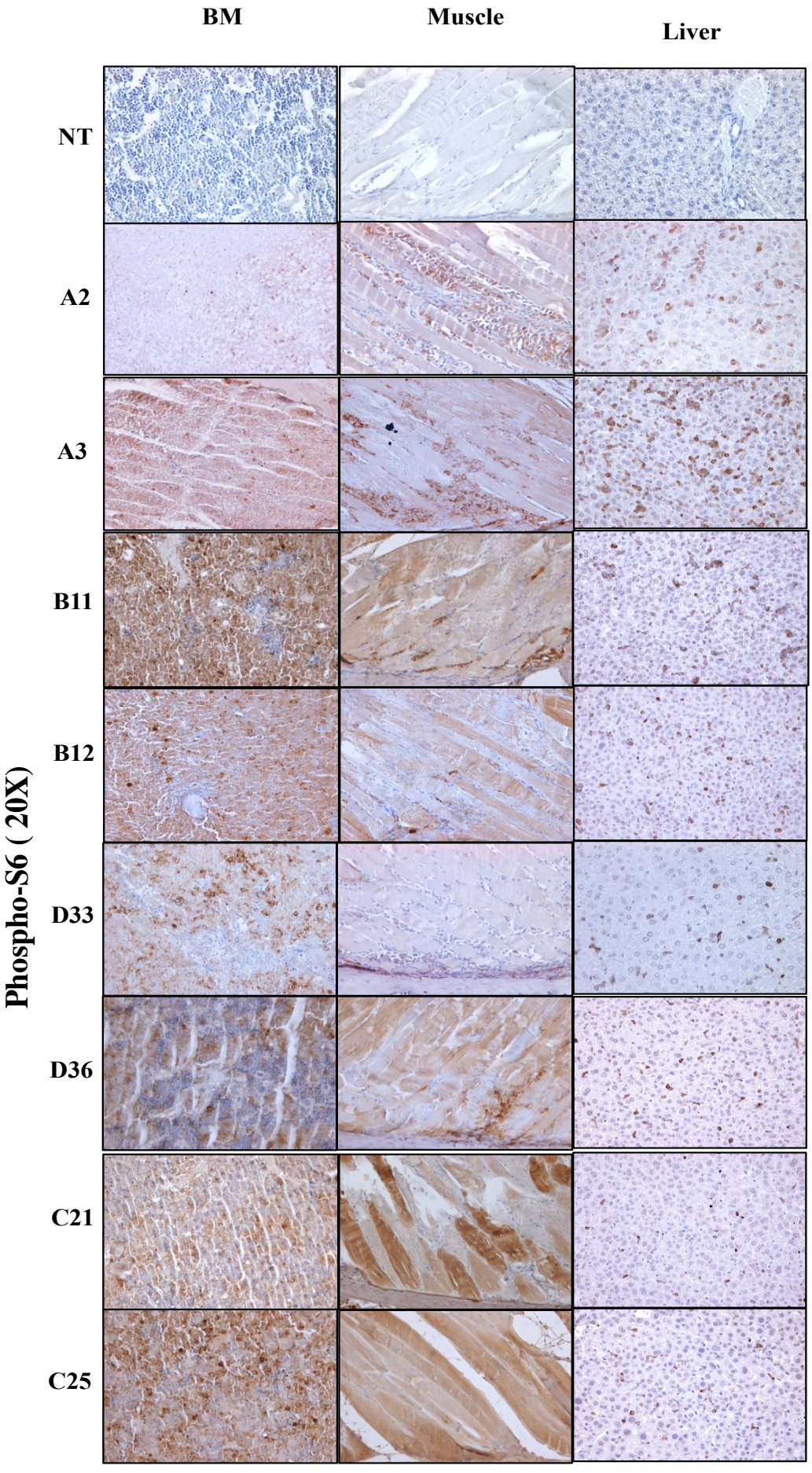

Legends of Supplemental Figures

Figure.S1. Heterogeneous responses of AML cells to LSD1 inhibitor-based therapy correlates with mTORC1 activity.

A) Metabolic activity or viability (cellular ATP %) of AML cell lines (SKNO-1, KASUMI-1, UF1, NB4, OCI-AML3 and THP-1 cells) following 6 days of treatment using varying concentrations of DDP38003 (0.0625 – 1 μM) normalized to vehicle-treated cells was assessed using ATP Cell Titer-Glo™ assay (n=3).

B) Flowcytometry dot plots showing the effect of 6 days of vehicle or DDP38003 treatment on the viability/apoptosis of the indicated AML cells assessed by Annexin V/PI staining.

C) Heatmap representation of the transcript changes in a subset of LSD1 target genes analyzed using RNA-Seq (LY96: Lymphocyte antigen 96; CD86: T-lymphocyte activation antigen CD86; ID3: Inhibitor of DNA binding 3; ITGAM: Integrin Subunit Alpha M (CD11b); ACVR2A; Activin A Receptor Type 2A; PI16: peptidase inhibitor 16; KCTD12: Potassium Channel Tetramerization Domain Containing 12; MS4A4A: Membrane Spanning 4-Domains A4A; C14orf109; Chromosome 14 Open Reading Frame 109; FGD6: FYVE, RhoGEF And PH Domain Containing 6) in THP-1 and KASUMI-1 cells following their treatment with vehicle or DDP38003. Values are row-scaled.

D-E) Growth curves of SKNO-1 (**D**) and NB4 (**E**) cells treated with either vehicle (DMSO) or MC2580 (2 μM) for the indicated time points of treatment assessed using trypan blue cell counting. Data were statistically analyzed using two way ANOVA followed by Bonferroni *post-hoc* test,[a]: $P < 0.05$ compared to vehicle-treated cells (n=3).

F-G) Western blot analysis of lysates obtained from SKNO-1 (**F**) and NB4 (**G**) cells 6 days after their treatment with either vehicle (DMSO) or MC2580 (2 μM). Vinculin served as the loading control.

Figure.S2. Mimicking energetic or nutritional stress using the non-metabolizable glycolytic inhibitor - 2-deoxyglucose - inhibits mTOR and reverses the resistance of AML cells to LSD1 inhibition.

A) Cell growth curve of THP-1 cells treated with vehicle or DDP38003 (0.5 μM) or 2DG (5 mM) or their combination for the indicated time points. Data were statistically analyzed using

two way ANOVA followed by Bonferroni *post-hoc* test, [a,b,c]: $P < 0.05$ compared to vehicle, DDP38003 or 2DG treated cells respectively (n=3).

B) Western blot analysis of lysates obtained from (**A**) after 72h of treatment. Vinculin served as the loading control.

C) Viability (cellular ATP%) of THP-1 cells following their treatment with varying concentrations of 2-deoxyglucose (2-DG) together with either vehicle (PEG) or DDP38003 (0.1 or 0.5 μM) assessed using Cell Titer-Glo™ assay. Data were statistically analyzed using two way ANOVA followed by Bonferroni *post-hoc* test, [a,b]: $P < 0.05$ compared to vehicle or DDP38003 (0.1 or 0.5 μM) treated cells respectively (n=3).

Figure.S3. mTOR inhibition augments the anticlonogenic activity of LSD1 inhibition further promoting myeloid differentiation of THP-1 cells in methylcellulose semisolid culture assays.

A) Percent of the number of THP-1 colonies treated with either vehicle, DDP38003 (DDP: 0.5 μM), AZD8055 (AZD: 10 nM) or their combination. Data were statistically analyzed using one way ANOVA followed by Bonferroni post-test, [*]: $P < 0.05$ compared to vehicle-treated cells.

B) Upper panel: Representative images of THP-1 colonies in semisolid culture with the indicated inhibitors. Lower panel: Representative images of cytospin preparations of THP-1 cells recovered at the end of the semisolid culture assay and stained with May Grunwald Giemsa stain.

Figure.S4. Abrogating mTOR signalling reverses the acquired resistance of primarily sensitive AML cells to LSD1 inhibition.

A) Schematic outline illustrating the method of generating LSD1i-resistant KASUMI-1 (designated as KASUMI-1/R) subline from the parental LSD1i-sensitive KASUMI-1 (KASUMI-1/P) cells.

B-C) Cell viability (Cellular ATP levels %) of LSD1i-naive KASUMI-1/P (P) and resistant KASUMI-1/R (R) cells following their treatment using varying concentrations of (**B**) DDP38003 (0.015–1μM) or (**C**) MC2580 (0.078–5μM) for 72h was assessed using Cell Titer-Glo™ assay (n=3). Data were statistically analyzed using two way ANOVA followed by Bonferonni post-test, [a]: $P < 0.05$ compared to parental KASUMI-1 (KASUMI-1/P) cells.

D) Immunoblot analysis of lysates obtained from LSD1i-naive KASUMI-1/P and resistant KASUMI-1/R cells 72h following their treatment using either vehicle or DDP38003 (0.5 μM). β-actin served as the loading control.

E-F) Cell viability (Cellular ATP levels %) of LSD1i-naive KASUMI-1/P and resistant KASUMI-1/R cells was determined 72h after their treatment with varying concentrations of either AZD8055 (**E**) or rapamycin (**F**) using Cell Titer-Glo™ assay (n=3). Data were statistically analyzed using two way ANOVA followed by Bonferonni post-test, [a]: $P < 0.05$ compared to parental KASUMI-1 (KASUMI-1/P) cells.

G) Percent of early (Annexin V^+/PI^-) and late (Annexin V^+/PI^+) apoptotic cells of KASUMI-1/P and KASUMI-1/R treated as indicated with either vehicle (Veh), DDP38003 (DDP) and/or AZD8055 (AZD) and analyzed using Annexin V/PI staining by flowcytometer. [*]: $P < 0.05$.

Figure.S5. Effect of LSD1 inhibition on AMP-activated protein kinase (AMPK) signalling and Raptor level in AML cells.

A-D) Western blot analysis of lysates obtained from THP-1 (**A**), KASUMI-1 (**B**), NB4 (**C**) and OCI-AML3 (**D**) cells 144h following their treatment with vehicle or DDP38003 (0.1 and 0.5 μM). Vinculin served as the loading control. The presented blots are derived from replicate samples run on parallel gels and controlled for even loading.

E-G) Western blot analysis of lysates obtained from THP-1 (**E**), SKNO-1 (**F**) and OCI-AML3 (**G**) cells 144h following their treatment with vehicle or DDP38003 (0.5 μM). β-actin served as the loading control.

Figure.S6.Activation of extracellular-signal regulated kinases 1 and 2 (ERK1/2) contributes to mTOR activation in resistant AMLs following LSD1 inhibition.

A-B) Western blot analysis of lysates obtained from sensitive KASUMI-1 (**A**) and resistant THP-1 (**B**) cells after 6 and 24h respectively of their treatment with either vehicle or DDP38003 (0.5 μM). Vinculin was used as the loading control. The presented blots are derived from replicate samples run on parallel gels and controlled for even loading.

C)Western blot analysis of lysates obtained from NB4 cells treated with vehicle or DDP38003 (0.1 and 0.5 μM) for 72h. Vinculin served as the loading control.

D) Western blot analysis of lysates obtained from THP-1 cells treated as indicated for 72h. β-actin served as a loading control.

E) Cell growth curves of THP-1 cells treated with vehicle, DDP38003, the selective MEK1/2 inhibitor U0126 (2.5 μM), and combination of DDP38003 and U0126. Data were statistically analyzed using two way ANOVA followed by Bonferroni *post-hoc* test, ^{a,b,c}: $P < 0.05$ compared to vehicle, DDP38003 or U0126 alone treated cells respectively (n=3).

F-H) Cell viability (Cellular ATP levels %) of NB4 (**F** and **G**) and OCI-AML3 (**H**) cells following their treatment with the indicated concentrations of pimasertib or trametinib (**C**) was assessed using Cell Titer-Glo™ assay.

Figure.S7.Genome-wide transcriptome analysis of KASUMI-1 and THP-1 cells following LSD1 inhibition.

Top enriched biological pathways categorized in physiological system, development and function (**A**) and molecular and cellular function (**B**) analysed by Ingenuity Pathway Analysis of differentially expressed genes (DEG) of KASUMI-1 and THP-1 cells 72h following LSD1 inhibition using DDP38003 (0.5 μM). P values were determined using Fisher exact test.

Figure.S8. LSD1 binding to insulin receptor substrate 1 (IRS1) promoter regions in AML cells.

A) Western blot analysis of lysates obtained from transduced KASUMI-1 cells expressing the indicated shRNAs. β-actin served as a loading control.

B) Tracks of LSD1 chromatin immunoprecipitation sequencing (LSD1 ChIP-Seq) at IRS1 promoter in NB4, KASUMI-1 and SKNO-1 AML cells (KASUMI-1 and SKNO-1 tracks were obtained from the cistrome database: Mcgrath *et al.,* 2016).

C-D) LSD1 ChIP-qPCR analyses were performed in NB4 (**C**) and OCI-AML3 (**D**) cells. Enrichment values at the indicated sites (A–D) were normalized against input DNAs. Values are means ± SD. *: $P < 0.05$.

E) H3K4me2 ChIP-qPCR analyses were performed in THP-1 cells 72h following their treatment with either vehicle or DDP38003 (0.5 μM). Enrichment values at the indicated sites (A–D) were normalized to input DNAs. Values are means ± SD. *: $P < 0.05$.

F) Tracks of H3K4me2 chromatin immunoprecipitation sequencing (H3K4me2 ChIP-Seq) on IRS1 gene in KASUMI-1 cells 72h following their treatment with vehicle or irreversible LSD1 inhibitors (GSK690 or RN-1) (From cistrome database deposited by Mcgrath et al., 2016).

Figure.S9. ATRA reverses LSD1i-induced IRS1 upregulation sensitizing resistant AML cells to LSD1 inhibition.

A-B) Normalized IRS1 mRNA levels assessed in THP-1 cells following their treatment with either vehicle (Veh) or ATRA (1 μM) for 72h and using two different primers (**A** and **B**) analyzed using RT-qPCR. Data were statistically analyzed using either Student's t test *: $P < 0.05$.

C) Western blot analysis of lysates obtained from NB4 cells following their treatment with either vehicle (Veh) or ATRA (1 μM) for 72h. β-actin served as a loading control.

D-E) Normalized IRS1 mRNA levels assessed in NB4 cells following their treatment with either vehicle (Veh) or ATRA (1 μM) for 72h and using two different primers (**D** and **E**) analyzed using RT-qPCR. Data were statistically analyzed using either Student's t test. *: $P < 0.05$.

F-G) H3K4me2 (**F**) and H3K27Ac (**G**) ChIP-qPCR analyses were performed in NB4 cells 72h following their treatment with either vehicle or ATRA (1 μM). Enrichment values at the indicated sites (A–D) were normalized to input DNAs. Values are means ± SD. *: $P < 0.05$.

H) Relative cell number of OCI-AML3 cells treated with vehicle or DDP38003 (0.5 μM) or all-trans retinoic acid (ATRA) or their combination. Data were statistically analyzed using one way ANOVA followed by Bonferonni *post-hoc* test,*: $P < 0.05$ (n=3).

I) Normalized IRS1 mRNA levels of OCI-AML3 cells treated as indicated in (**H**) assessed using RT-qPCR. Data were statistically analyzed using one way ANOVA followed by Bonferonni *post-hoc* test,*: $P < 0.05$.

Figure.S10. Effect of LSD1 inhibition using DDP38003 on primary human CD34^{+} cord blood cells.

A) Effect of DDP38003 treatment (0.3 μM) on the proliferation of primary human CD34^{+} cord blood cells assessed using trypan blue cell counting (n=3).

B) Metabolic activity or viability (ATP %) of primary human $CD34^+$ cord blood cells treated with vehicle or DDP38003 (0.3 μM) for 72h assessed using Cell Titer-Glo™ assay (n=3).

C) Western blot analysis of primary human $CD34^+$ cord blood cells treated with vehicle or DDP38003 (0.3 μM) for 72h. Vinculin served as the loading control.

Figure.S11. Effect of LSD1 inhibition on primary human $CD34^+$ cord blood cells transduced with lentiviral vector expressing human MLL-AF9 ($hCD34^+$ MLL-AF9).

A) Effect of DDP38003 treatment (0.5 μM) on the proliferation of $hCD34^+$ MLL-AF9 cells assessed using trypan blue cell counting (n=3). Data were statistically analyzed using two way ANOVA followed by Bonferonni post-test. *: $P < 0.05$.

B-C) Normalized CD11b (**B**) and CD86 (**C**) mRNA levels assessed in $hCD34^+$ MLL-AF9 cells 6 days following their treatment with either vehicle or DDP38003 (0.5 μM). Data were statistically analyzed using Student's t test.*: $P < 0.05$ compared to vehicle-treated cells.

D) Western blot analysis of lysates obtained from $hCD34^+$ MLL-AF9 cells 6 days following their treatment with either vehicle or DDP38003 (0.5 μM). β-actin served as the protein loading control.

E-F) Relative number of coarse (**E**) and disperse (**F**) colonies of $hCD34^+$ MLL-AF9 cells treated as with either vehicle, MC2580 (2 μM) or DDP38003 (0.5 μM) and cultured in semisolid medium (n=3). Data were statistically analyzed using either one way ANOVA followed by Bonferrroni *post-hoc* test *: $P<0.05$ compared to vehicle-treated cells.

G) Representative phase contrast images of $hCD34^+$ MLL-AF9 colonies treated as indicated (first column) and their cytospin preparations recovered at the end of the semisolid culture assay and after being stained with May Grunwald Giemsa stain (2^{nd} and 3^{rd} columns). Red arrows refer to macrophages.

Figure.S12.Inhibiting mTOR sensitizes primary human MLL-AF9 expressing (AML-IEO20) leukemia cells to LSD1 inhibition.

A-B) Cell cycle analysis (**A**) and percent of apoptotic cells (**B**) of patient-derived AML-IEO20 leukemic cells following their treatment with either vehicle (designated as V),

DDP38003 (D), rapamycin (referred to as R) or AZD8055 (referred to as A) analyzed using FACS analysis.

C) May Grunwald-Giemsa stained blood smear as well as cytospin preparations of spleen and bone marrow obtained from AML-IEO20 transplanted NSG mice 15 days after initiating treatment with vehicle or DDP38003 or rapamycin or a combination of DDP38003 and rapamycin (20 and 40x).

D) Histopathological examination of the spleen, bone marrow as well as muscular tissues harvested from non-transplanted NSG mice (NT) as well as mice xenotransplanted with AML-IEO20 leukemia 15 days after initiating treatment with vehicle (#A2 and #A3), DDP38003(#B11 and #B12), rapamycin (#D33 and #D36) or a combination of DDP38003 and rapamycin (#C21 and #C25).

E) Immunohistochemical assessment of human nuclei in the spleen, bone marrow as well as muscular tissues harvested from non-transplanted NSG mice (NT) as well as mice xenotransplanted with AML-IEO20 leukemia 15 days after initiating treatment with vehicle (#A2 and #A3), DDP38003(#B11 and #B12), rapamycin (#D33 and #D36) or a combination of DDP38003 and rapamycin (#C21 and #C25).

F) Immunohistochemical assessment of ribosomal S6 phosphorylation as a readout of mTORC1 activity in the bone marrow as well as muscular tissues harvested from non-transplanted NSG mice (NT) as well as mice xenotransplanted with AML-IEO20 leukemia 15 days after initiating treatment with vehicle (#A2 and #A3), DDP38003 (#B11 and #B12), rapamycin (#D33 and #D36) or a combination of DDP38003 and rapamycin (#C21 and #C25).